AD-777 462

LOCAL STRESS-STRAIN APPROACH TO CUMULATIVE FATIGUE DAMAGE ANALYSIS

JoDean Morrow, et al

Illinois University

Prepared f r:

Naval Air Development Center

January 1974

FOREWORD

This report summarizes more than five years of research on the problem of estimating the fatigue life of spectrum loaded members. Three cooperative research contracts between the Aero Structures Department of the Naval Air Development Center and the H. F. Moore Fracture Research Laboratory of the Department of Theoretical and Applied Mechanics of the University of Illinois, at Urbana, made this investigation possible. The most recent of these was Contract No. N00156-70-C-1256 and this report constitutes the final report for that contract. Background research was performed under Contract Nos. N-156-46083 and N00156-67-C-1875. Messrs. M. S. Rosenfeld, R. E. Vining and F. F. Borriello were instrumental in inaugurating this line of research and provided technical liaison for the Navy.

A number of staff members and graduate students have made valuable contributions to the procedure for cumulative fatigue damage analysis which is outlined in this report. An attempt is made in the text to acknowledge the individuals and their contributions by citing their published works. Those papers that were produced as a part of this program are indicated by an asterisk in the list of references: Refs. (1-18).

UNCLASSIFIED

Security Classification

AD 777462

DOCUMENT CONTROL DATA - R & D

Security classification of title, body of abstract and indexing annotation must be entered when the overall report is classified)

1. ORIGINATING ACTIVITY (Corporate author) Department of Theoretical and Applied Mechanics University of Illinois Urbana, Illinois 61801	2a. REPORT SECURITY CLASSIFICATION Unclassified 2b. GROUP ---

3. REPORT TITLE

Local Stress-Strain Approach to Cumulative Fatigue Damage Analysis

4. DESCRIPTIVE NOTES (Type of report and, inclusive dates)
Final Report (26 September 1969 to 21 June 1971)

5. AUTHOR(S) (First name, middle initial, last name)

JoDean Morrow, J. F. Martin and N. E. Dowling

6. REPORT DATE April 1973 (Printed January 1974)	7a. TOTAL NO. OF PAGES 78	7b. NO. OF REFS 48
8a. CONTRACT OR GRANT NO. NOO156-70-C-1256 b. PROJECT NO. c. d.	9a. ORIGINATOR'S REPORT NUMBER(S) T & A M Report No. 379 9b. OTHER REPORT NO(S) (Any other numbers that may be assigned this report) None	

10. DISTRIBUTION STATEMENT
Approved for public release--distribution unlimited.

11. SUPPLEMENTARY NOTES ---	12. SPONSORING MILITARY ACTIVITY Aero Structures Department Naval Air Development Center Johnsville, Warminster, Pa. 18974

13. ABSTRACT

A cumulative fatigue damage procedure for estimating the fatigue crack initiation life of notched structural members subjected to known load histories is outlined. This procedure assumes that a knowledge of the local cyclic stress-strain response of the metal at the most severely strained region in a member is sufficient to predict when a crack will form there. Some of the steps in this procedure that are of current interest and which are especially applicable to a local stress-strain approach are discussed. Alternative, approximate and/or abbreviated steps in the cumulative fatigue damage procedure are given wherever possible. Limitations of the method and areas where research is needed are pointed out.

Cumulative fatigue test results for smooth specimens, notched plates and built-up box beams are compared to life calculations made using the local stress-strain approach. Cyclic deformation and fracture properties, used in the analysis, were obtained from tests on a limited number of axially loaded unnotched specimens. These examples indicate that a cumulative fatigue damage analysis based on the local stress-strain approach employing a minimum amount of materials test data can be used to make reasonable life estimates for members similar to many practical structural members. While there appears to be no serious limitations on the complexity of load histories that can be analyzed, the fatigue analysis of parts with complex geometric form is presently impractical without direct measurements of critical strains in the part.

DD FORM 1 NOV 65 1473 (PAGE 1)

S/N 0101-807-6811

UNCLASSIFIED

Security Classification

A-31408

14 KEY WORDS	LINK A		LINK B		LINK C	
	ROLE	WT	ROLE	WT	ROLE	WT
Metal fatigue Cyclic stress-strain Stress concentration Strain cycling Cumulative fatigue damage Computer based fatigue analysis						

SUMMARY

A cumulative fatigue damage procedure for estimating the fatigue crack initiation life of notched structural members subjected to known load histories is outlined. This procedure assumes that a knowledge of the local cyclic stress-strain response of the metal at the most severely strained region in a member is sufficient to predict when a crack will form there. Some of the steps in this procedure that are of current interest and which are especially applicable to a local stress-strain approach are discussed. Alternative, approximate and/or abbreviated steps in the cumulative fatigue damage procedure are given wherever possible. Limitations of the method and areas where research is needed are pointed out.

Cumulative fatigue test results for smooth specimens, notched plates and built-up box beams are compared to life calculations made using the local stress-strain approach. Cyclic deformation and fracture properties, used in the analysis, were obtained from tests on a limited number of axially loaded unnotched specimens. These examples indicate that a cumulative fatigue damage analysis based on the local stress-strain approach employing a minimum amount of materials test data can be used to make reasonable life estimates for members similar to many practical structural members. While there appears to be no serious limitations on the complexity of load histories that can be analyzed, the fatigue analysis of parts with complex geometric form is presently impractical without direct measurements of critical strains in the part.

TABLE OF CONTENTS

	Page
FOREWORD	ii
SUMMARY	iii
LIST OF FIGURES	v
LIST OF SYMBOLS	vii
INTRODUCTION	1
LOCAL STRESS-STRAIN APPROACH	2
RELATING LOCAL AND NOMINAL STRESS-STRAIN BEHAVIOR	4
SMOOTH SPECIMEN STRESS-STRAIN BEHAVIOR	7
SMOOTH SPECIMEN FATIGUE BEHAVIOR	10
FATIGUE DAMAGE ANALYSIS	14
CONCLUSIONS, LIMITATIONS AND FUTURE DIRECTIONS	17
APPENDIX - COMPUTER BASED FATIGUE LIFE PREDICTIONS FOR NAVY BOX BEAMS	19
REFERENCES	28
FIGURES	

LIST OF FIGURES

No.	Title
1	Smooth Specimen Representation of Material at the Critical Zone
2	Cyclic Softening and Relaxation of Mean Stress under Neuber Control (Ti-8Al-1Mo-1V, K_f = 1.75), (12)
3	Cumulative Fatigue Damage Procedure
4	Recorded Data from a Smooth Specimen Simulation of the Local Stress-Strain Behavior of a Notch (1)
5	Stress-Strain Response of a Smooth Specimen Notch Root Simulation (7075-T6 Aluminum, K_f = 1.95), (12)
6	Stress-Strain Response of a Smooth Specimen Notch Root Simulation (7075-T6 Aluminum, K_f = 1.95), (12)
7	Comparison of Notched Fatigue Data with Life Curves Predicted from Smooth Specimen Data (6)
8	Distribution of Failure Predictions (12)
9	Stress-Strain Response for 2024-T4 Aluminum (11)
10	Hysteresis Loops at Varying Strain Amplitudes for Man-Ten Steel (27)
11	Typical Stress-Inelastic Strain Hysteresis Loops during a Test with Overstrains every 10^5 Cycles for SAE 4340 Steel (14)
12	Cyclic Relaxation of Mean Stress for 7075-T6 Aluminum (11)
13	Actual and Simulated Stress-Strain Response of 2024-T4 Aluminum
14	Representation of Elastic, Plastic and Total Strain Amplitude-Fatigue Life Relations
15	Inelastic Strain versus Life for SAE 4340 Steel (14)
16	Total Strain versus Life for SAE 4340 Steel (14)
17	Equivalent Strain Amplitude-Life Comparison for SAE 4340 Steel (10)
18	Stress-Strain Recording for Initial Overstraining
19	Stress versus Life for SAE 4340 Steel (14)
20	Mean Stress Data for SAE 4340 Steel Compared to Eqs. 11 and 12

No.	Title
21	Distribution of Failure Predictions for 2024-T4 Aluminum (15)
22	Distributions of Life Calculations for SAE 4340 Steel (14)
23	Load-Life Curve for Plates Subjected to Load Spectra Shown (11)
24	Constant Amplitude Box Beam Predictions and Data: 1g to P_{max} Loading
25	Constant Amplitude Box Beam Predictions and Data: 1g ± P Loading
26	Constant Amplitude Box Beam Predictions and Data: - 1g to P_{max} Loading
27	Load Spectrum B Box Beam Predictions and Data
28	Box Beam Specimen Design
29	Highly Stressed Area of Box Beam Cover Plate
30	Strain Spectrum for One Specimen Simulation
31	Monotonic Stress-Strain Curve of 7075-T6 Aluminum
32	Set of Stable Hysteresis Loops for Determining the Cyclic Stress-Strain Curve
33	Plastic Strain versus Stress Amplitude for 7075-T6 Aluminum
34	Cyclic Relaxation Data for a Strain Range from 0.0 to -0.0155 for 7075-T6 Aluminum
35	Strain-Life Data for 7075-T6 Aluminum
36	Rheological Model for Computer Simulation
37	Model Approximation of Stress-Strain Curve
38	Example of Cyclic Hardening Used in the Model
39	Flow Chart of Computer Program

LIST OF SYMBOLS

α	Material constant indicating sensitivity to mean stress
b	Fatigue strength exponent
b_n	Minimum width of a notched specimen
c	Fatigue ductility exponent
d	Material constant
E	Modulus of elasticity
E_s	Secant modulus for the metal at a notch root
E_∞	Secant modulus for the metal away from a notch root
E_i^σ	Stiffness of i^{th} spring, superscript σ signifies stress dependence
E_i	Constant relating to i^{th} spring
E_i^*	Effective modulus of i^{th} segment of stress-strain curve
e, Δe	Nominal strain, nominal strain range
ϵ, $\Delta\epsilon$	True strain, true strain range
ϵ_f	True fracture ductility
ϵ_f'	Fatigue ductility coefficient
ϵ_p, $\Delta\epsilon_p$	Plastic strain, plastic strain range
$\Delta\epsilon_r$	Equivalent completely reversed strain range
ϵ_i^*	Maximum strain attained over i^{th} segment of stress-strain curve
$\delta\epsilon_i$	Change in strain over i^{th} element
$\delta\epsilon_i^*$	Change in strain over i^{th} segment
K', K*	Cyclic strength coefficient, transient strength coefficient
K_t	Theoretical elastic stress concentration factor
K_σ	Stress concentration factor
K_ϵ	Strain concentration factor
K_f	Fatigue notch factor

M	Constant in relaxation function
N_f	Number of cycles to failure
$2N_f$	Reversals or half cycles to failure for a constant amplitude test
N_{fi}	Life for a given strain amplitude and mean stress
$2N_t$	Transition fatigue life
n_i	Number of cycles at a given strain amplitude and mean stress
n^*, n'	Transient strain hardening exponent; n' is the stable value
P	Load
r	Notch radius
$S, \Delta S$	Nominal stress, nominal stress range
S_u	Ultimate tensile strength
$\sigma, \Delta\sigma$	True stress, true stress range
σ_f'	Fatigue strength coefficient
σ_f	True fracture strength
σ_a, σ_o	Stress amplitude, mean stress
σ_{max}	Maximum stress
σ_r	Equivalent completely reversed stress amplitude
$\bar{\sigma}_i$	Constant stress exerted by i^{th} frictional slider
σ_i	Residual stress exerted by i^{th} spring
σ_f^*	Final stress attained for a particular reversal
σ_i^*	Maximum stress attained over i^{th} segment of stress-strain curve
$\delta\sigma_i^*$	Change in stress for i^{th} segment for stress-strain curve
t	Specimen thickness
V_n	Highly stressed volume for notched specimen
V_u	Highly stressed volume for unnotched specimen

INTRODUCTION

More than 100 years of research on the subject of metal fatigue has been concerned primarily with the effect of the many factors influencing fatigue damage. A number of specific practical problems have been solved and much has been learned about the basic mechanisms of the fatigue process. However, only limited progress has been made toward developing procedures that can be used to estimate fatigue lives of components still in the design or development stage. In most cases, it is necessary to subject a trial design of a component to simulated service testing or to rely heavily upon actual service experience for similar parts. Component testing and the collecting of service data are expensive and time consuming. It is desirable, therefore, that these activities be augmented by analytical procedures for calculating fatigue lives.

It has been clearly established for some time that local repeated plastic strain is responsible for fatigue damage. Yet, the engineering approach to fatigue problems has usually been to consider the nominal stresses caused by the maximum forces, moments and/or torques acting on a part. "Stress" calculations are usually based on the assumption that the material responds in a linear elastic fashion.

The research discussed here is based on the premise that an understanding of the cyclic stress-strain behavior and fatigue resistance of the material at the most highly strained region in a member should be sufficient to predict when that region will fail by fatigue. Fatigue damage generally nucleates in the root of the most severe notch in a region of high cyclic nominal stress. An extension of this simple approach to elements ahead of the crack, once it is formed, could be applied to improve understanding of fatigue crack propagation. This coupled with the fracture mechanics concept of an unstable fast crack could provide an analytic basis for the entire fatigue sequence of crack initiation, propagation and final fracture. Here we have not separated the initiation, propagation and fracture stages of fatigue. Instead our efforts have been concentrated on arriving at the materials and mechanics concepts needed to predict when one small element of metal will fail by fatigue.

For the sake of simplicity, many factors that may have a large effect on the fatigue life of a member in service have been ignored. Amongst these are the effects of temperature, corrosion, machining and fabrication stresses and multiaxial states of stress which may be present at the local point where cracks initiate.

Purpose and Scope

The aim of this final report is to outline a procedure for cumulative fatigue damage analysis which has evolved at Illinois and elsewhere over the past several years. During this period rapid progress has been made in fatigue analysis, particularly in the areas of better characterizing the cyclic deformation and fatigue resistance of metals and in applying high speed computers to do the extensive bookkeeping necessary in a fatigue damage analysis. We will draw mainly from our own work and experience and that of close associates. Examples are given at the end of the paper to illustrate the application of current fatigue analysis techniques. Finally, the weak points in the procedure which need additional systematic research are enumerated and briefly discussed

LOCAL STRESS-STRAIN APPROACH

The cyclic stress-strain response and the fatigue resistance of a metal may be characterized by performing a series of laboratory tests on smooth uniaxial specimens. A member made of this metal may be analyzed for fatigue resistance by considering the behavior of the material at the site of crack initiation to be analogous to the response of a smooth specimen subjected to the same cyclic strains. The basic idea of this approach is depicted in Fig. 1 for a simple notched plate. It is assumed that the critical zone is in an uniaxial stress state and that the smooth specimen is representative of the metal where fatigue cracks initiate.

To estimate the fatigue crack initiation life of structural components, the local cyclic stresses and strains affecting the critical zone must be related by the methods of mechanics to the known load or nominal stress history on the part. In practice, this requirement is perhaps the most difficult to fulfill because of the geometric complexity of most structural parts and because the critical location usually experiences cyclic plastic deformation.

Mechanics methods for elasto-plastic analysis of structural components subjected to cyclic loading have not as yet developed to the level required for cycle to cycle determinations of local stresses and strains in complex parts. As an alternative, experimental stress analysis techniques can be used in some cases. However, even if the component has been fabricated and the type of loading experienced in service simulated, strain gages may only be useful for measuring the nominal strains since the location of the critical region may be unknown or may be so small or inaccessible that meaningful strain measurements are impractical.

Simple Notched Members

The viability of the local stress-strain approach to fatigue damage analysis has been demonstrated for simple notched members such as shown in Fig. 1. For such members the local and nominal stresses and strains can be related by an elasto-plastic "strength of materials" type of analysis based on work by Neuber (19). Details of this analysis are given in the next section. The analysis provides a rule that specifies the cyclic stress-strain control conditions necessary to simulate on a smooth specimen the constraint of the material surrounding the metal at a notch root in a member subjected to a known load history.

An example of this type of control is shown in Fig. 2. This is an actual X-Y plot of the stress-strain response of a smooth specimen controlled according to Neuber's rule to simulate the material response at the root of a notch in a plate subjected to a zero to tension load history. Although the nominal stress on the plate is always tensile (see the inset in Fig. 2), the local stress at the notch root is seen to cyclically shift toward compression tending toward completely reversed local stress. The local strain is seen to cyclically increase in the tensile direction.

The cycle-dependent relaxation of stress, cyclic hardening, softening, effects of overload on a notched member and other factors which will affect its fatigue crack initiation life can be simulated on smooth specimens using this technique (12). In addition, the specimen is subjected to cumulative fatigue damage at the same rate

as at the notch root in the simulated member. Thus, the fatigue life of the smooth specimen should be nearly equal to the crack initiation life of the simulated notched member. In Ref. (12) it is shown that the simulated smooth specimen lives agree with actual notched specimen lives within about a factor of two in most cases.

Computer Based Simulation

A major objective of the fatigue damage procedure reviewed in this report is to eliminate the need for extensive testing and to reduce the time and expense necessary for evaluating the fatigue life of structures subjected to large numbers of cycles and complicated load spectra. The type of smooth specimen simulation test just described is time consuming and requires sophisticated testing apparatus and personnel. In fact, only simple loading sequences can be simulated at the present time. A more practical and efficient approach can be employed by "simulating" the smooth specimen simulation using a high speed digital computer. Martin et al. (11) have demonstrated the feasibility of this approach.

The necessary materials properties for the metal of interest are estimated from other properties and taken from the literature and/or various "data banks" that are now becoming available. If vital materials information is not available, minimal smooth specimen testing may be necessary to fully characterize the cyclic deformation and fracture resistance of the metal.

Cyclic as well as monotonic properties of the metal of which the member is made are needed since the stress-strain response of most metals changes significantly during cyclic straining into the plastic range. These properties along with a digital computer model permit the cycle to cycle response of the material to be rapidly evaluated for virtually any history of input.

Once the cyclic stress-strain properties of the metal are embodied in the computer model, a method of estimating the local stresses and strains from the load history on a member can be employed in the computer. Of the available methods, Neuber's rule seems to be the most practical for a notched member. At present, however, the effects of geometry and notch size are treated in the Neuber analysis by means of a fatigue notch factor, K_f. For small notches, complicated shapes or welds, K_f is difficult to estimate without fatigue testing of actual parts.

From the computed local stresses and strains, fatigue damage or expected life can be calculated if strain amplitude and mean stress versus fatigue life information are available for the metal of interest. Such information requires appropriate fatigue testing or can be estimated from other known properties. Local fatigue damage may be assayed for each reversal or half cycle of strain via a cycle counting method, or by properly summing the damage due to small increments of the stress-strain history in conjunction with the computer model of the cyclic response. Of the well known cycle counting methods, only the range pair and rain flow methods give rational counting results if there are minor cycles superimposed on changes in the mean level.

The cumulative fatigue damage analysis procedure which is briefly described above is outlined in the schematic shown in Fig. 3. Steps in the procedure will be discussed in more detail in the next four sections and an example of the application of this method to estimate the fatigue life of Navy box beams is presented in the Appendix.

RELATING LOCAL AND NOMINAL STRESS-STRAIN BEHAVIOR

If the most highly stressed location in a component subjected to variable loading is known, it may be possible in some situations to mount a strain gage at that location. In this way a record is obtained of the strain history for a typical duty cycle or period of usage of the vehicle, machine, or aircraft of which the component is a part. The number of repetitions of this strain history required for crack initiation can then be estimated, provided the state of stress at the critical location can be treated as uniaxial and its cyclic value can be estimated so that the effect of mean stress on fatigue damage can be included in the analysis.

If a suitable test facility is available, the known strain history can be enforced upon an axially loaded unnotched specimen until it fails. Thus it is possible to obtain a direct estimate of the fatigue life which bypasses all of the analysis. Alternatively, the stress history from the smooth specimen test could be measured during a representative block of the strain history and the results used to calculate the fatigue life taking into account the effects of mean stress. In this way the specimen need not be tested to failure.

If a computer based model is available that is capable of simulating the cyclic stress-strain response of the metal, the stress history corresponding to the known strain history can be determined so that a life estimate can be made. Such models have been developed by Martin et al. (11,20) and may include the effects of cyclic hardening or softening and cyclic relaxation of mean stress.

Some Possible Simplifications in Fatigue Analysis

For a typical section of strain history measured on a component, it is reasonable to assume, provided there has been a period of shakedown, that the material behavior is nearly stable or that the cyclic hardening or softening is no longer significant. The fatigue damage procedure may therefore be simplified. Cyclic relaxation of mean stress and cyclic creep can often be omitted from the model since these will not affect fatigue life calculations significantly unless there are long periods of nearly constant cyclic strain amplitude present in the history.

If the strain history is simple or short and if cyclic hardening/softening, relaxation, and creep can be neglected the stable cyclic stress-strain curve of the metal may be used to graphically estimate the stress response. It is necessary to know the residual stress at the beginning of a period of typical strain history only if the typical history does not include at least one strain cycle large enough to set up a system of residual stresses that "override" the initial residual stresses (18).

If most of the fatigue damage is due to sufficiently large strain cycles, the mean stress present during these cycles will be insignificant due to cyclic plasticity and may be neglected in the fatigue damage analysis. It may be determined if mean stress can be neglected by making trial damage calculations using life data for zero mean stress. The results of this calculation can then be compared to the cyclic stress-strain curve to determine what fraction of the calculated damage is due to cycles during which no significant mean stress would be expected to be present. If this fraction is large, the life estimate will not be significantly affected by the mean stresses during any smaller cycles which might be present and mean stress can be neglected.

Neuber Analysis

Usually the cyclic strains cannot be measured at the fatigue crack initiation site in a member. Rather, nominal strains are measured near to the critical location or the applied external forces are measured and nominal stresses are calculated. In either case, a mechanics analysis of the member must be performed to relate the nominal values to the local stresses and strains.

Several types of notch analyses (6, 19, 21, 22) have been proposed for relating nominal and local cyclic stresses and strains. Most of the applications have been for constant amplitude or block type loading. Also, the components which have been tested were usually laboratory samples. Few fatigue analyses have been performed on components subjected to realistic load spectra (23).

Neuber's rule (19) provides a relation between local strain and stress concentration factors and the theoretical stress concentration factor.

$$K_t = (K_\epsilon K_\sigma)^{\frac{1}{2}} \tag{1}$$

where K_ϵ, K_σ, and K_t are the local strain, local stress and theoretical elastic stress concentration factors, respectively. This relation was modified for fatigue applications (6) into the following form:

$$K_f(\Delta S\, \Delta e\, E)^{\frac{1}{2}} = (\Delta\sigma\, \Delta\epsilon\, E)^{\frac{1}{2}} \tag{2}$$

where E is the elastic modulus, ΔS and Δe are the nominal stress and strain ranges, $\Delta\sigma$ and $\Delta\epsilon$ are the local stress and strain ranges, and K_f is the fatigue notch factor. With the exception of the change of K_t to K_f, Eq. 2 is derived from the definitions of the terms in Eq. 1. The substitution of K_f for K_t is necessary to correct for size effects in fatigue, especially when the notch is small (16, 17).

If the loads are small enough that the behavior of the notched member is nominally elastic, i.e., $\Delta S/\Delta e = E$, Neuber's rule reduces to

$$\frac{(K_f \Delta S)^2}{E} = \Delta\sigma\, \Delta\epsilon \tag{3}$$

also

$$K_f \Delta S = (\Delta\sigma\, \Delta\epsilon\, E)^{\frac{1}{2}} \tag{3a}$$

Equations 2 and 3 imply that the material surrounding the critical zone imposes both a strain and stress restriction on the material there. This would seem reasonable in that the surrounding material neither acts as a rigid wall nor does it simply load the highly stressed region.

Another expression relating local and nominal behavior that is based on Stowell's work (22) has been proposed for use in cyclic analyses (24)

$$\sigma = S(1 + (K_t - 1)\frac{E_s}{E_\infty}) \quad (4)$$

where E_s is the secant modulus at the stress raiser and E_∞ is the secant modulus for the material far removed from the stress raiser. In Ref. (24) this relation is successfully employed to predict the local cyclic stresses near the notch root of edge notched plates. For these predictions it was necessary to determine the stress-strain behavior of the material from smooth specimens. However, fatigue predictions were not made using Eq. 4 and smooth specimen fatigue data.

Manson and Hirschberg (25) discuss both the Neuber and Stowell equations, but only Neuber's relation was used to make life predictions. Few comparisons between experimentally and analytically determined stresses and strains at the notch root have been made.

Wetzel (1) used Neuber's relation to estimate the experimental data of Ref. (24). Agreement was also good. Most applications of Neuber's rule have concerned predicting fatigue lives. These life predictions are made either by subjecting a smooth specimen to control conditions which obey Eq. 3 for the nominal stresses on the simulated notched specimen or by using Eq. 3 for each reversal along with smooth specimen stress-strain and fatigue data.

Examples of the Applications of Neuber's Rule

Wetzel (1) manually controlled the stress and strain limits on smooth specimens so as to obey Neuber's rule for zero to tension loading of notched plates. Figure 4 shows a typical result from these tests.

Attempts to enforce Neuber control on smooth specimens by means of an analog computer have failed. However, digital computer control of a materials test system produced the results shown in Fig. 2 (12). Figures 5 and 6 illustrate the use of Neuber control to simulate the residual stresses produced by overloading notched members. For any type of notch simulation on a smooth specimen, the real time expended in determining failure can be quite large.

Topper, et al. (6) showed that completely reversed constant amplitude fatigue data for both smooth and notched specimens can be represented by a single band on the same life curve by employing Eq. 2. For notched members the left side of the equation is used as a life parameter. For smooth specimens the right side of the equation is used. Figure 7 is an example of the correlation that is possible using this approach. The line is based on smooth specimen data (points not shown) and the points are notched fatigue results.

Whether Stowell or Neuber equations are used to relate nominal to local stresses and strains, the stress-strain response of the metal of interest must also be employed in the analysis. This is done most directly by simulation testing of a smooth specimen. However, the sophistication needed in equipment and test technique is quite large. Stadnick and Morrow (12) listed fatigue predictions resulting from three different means of controlling the Neuber parameter. An approximate type of Neuber control that is suitable for an analog computer was used for some of the tests. It is termed "sliding line control." It approximates the hyperbolic form of Neuber's rule (see Fig. 4) by a straight line. The accuracy of the predictions reported in Ref. (12) is summarized in Fig. 8.

SMOOTH SPECIMEN STRESS-STRAIN BEHAVIOR

Since the relation between local and nominal behavior involves one equation and two unknowns, more information is needed relating local stress, σ, and strain, ϵ. Such a relation is derived from experimental data, most of which is from completely reversed strain or stress control. It is necessary to restrict the treatment to the uniaxial state of stress. Biaxial and triaxial cyclic deformation and fatigue behavior of metals have not been sufficiently investigated to allow their consideration. Fortunately, many practical situations involve an approximately uniaxial state of stress since the location where fatigue damage initiates is usually at a free surface.

Axially loaded unnotched specimens with cylindrical or hourglass shaped test sections are appropriate for studies of materials behavior. For such specimens it can be assumed that the states of stress and strain are nearly uniform, and also these quantities can be conveniently measured. More detailed information on testing techniques for such specimens is given in Ref. (7).

Static and Steady State Cyclic Stress-Strain Behavior

The most popular test for assessing mechanical resistance of a material is the monotonic (static) tension test. At least the engineering tensile properties that can be obtained from this test are listed for most structural metals in material handbooks. For this reason attempts are made to associate cyclic and monotonic properties (7). Such parameters as the true fracture strength, σ_f, true fracture ductility, ϵ_f, strain at necking, and the ultimate strength, S_u, can all be of use for making fatigue life estimations. Endo and Morrow (3) list the monotonic properties of the four aircraft metals of major interest in this investigation.

For most metals, the stable cyclic stress-strain curve is quite different from the monotonic. References (4) and (26) demonstrate this difference. Reference (4) also lists the cyclic properties of the four aircraft metals used here.

There are at least four ways of determining the cyclic stress-strain curve: 1) a curve passing through the tips of stable loops from companion specimens tested at different strain ranges, 2) the curve passing through the tips of loops from an incremental step strain test (4), 3) monotonic tension after a stable state has been obtained, and 4) analysis of the curves from stable individual hysteresis loop. The cyclic stress-strain curve in most cases will be quite different from the stress-strain curve obtained from a tension test. A mathematical expression for the cyclic stress-strain curve which is satisfactory for most engineering metals may be obtained if the cyclic strain is separated into its elastic and inelastic components.

$$\frac{\Delta\epsilon}{2} = \frac{\Delta\epsilon_e}{2} + \frac{\Delta\epsilon_p}{2} = \frac{\Delta\sigma}{2E} + \left(\frac{\Delta\sigma}{2K'}\right)^{\frac{1}{n'}} \qquad (5)$$

where the prime (') denotes cyclic, therefore, K' and n' are the cyclic strength coefficient and cyclic strain hardening exponent, respectively. The constants for Eq. 5 are usually determined as the slope and intercept of a log-log plot of cyclic stress amplitude and cyclic plastic strain amplitude.

By whatever means the cyclic stress-strain curve is determined, it is only useful if it can reproduce the actual cyclic stress-strain behavior of the material for which the constants were determined. Figure 9 is a plot of a set of stable hysteresis loops of 2024-T4 aluminum with the loop tips at a common origin (11). Equation 5 fits the data quite well. Figure 10 is the same type of illustration for a structural steel (27). For this steel the curve described by Eq. 5 does not fit the actual loop shape very accurately.

Cyclic Hardening and Softening

In a constant strain controlled test, cyclic hardening is observed as an increase in the stress range and softening as a decrease. Some of the hardening and softening characteristics of the metals of interest are discussed in Refs. (3) and (26). Morrow (28) cites some extreme examples of hardening and softening of copper. Dowling (14) observed cyclic softening of quenched and tempered SAE 4340 steel. An initially hard metal, such as 4340 steel, can progress from an elastic condition to a state resulting in significant inelastic strain while being cycled at a stress or strain range that initially produced only elastic behavior. Many structural steels have been observed to either harden or soften, depending on the strain range (29). Steels that are overstrained and then cycled at a low strain level may cyclically harden due to dynamic strain aging as seen in Fig. 11 for the SAE 4340 steel tested by Dowling (14).

Attempts have been made to predict whether a metal will harden or soften by the value of the monotonic strain hardening exponent, n (26, 28, 30). Metals with high initial n values tend to cyclically harden, while those with low values of n tend to soften.

If loop shape is to be described by an equation of the form of Eq. 5, for each loop during cyclic hardening or softening, the strength coefficient and/or the strain hardening exponent must be altered with each cycle. Martin, et al. (11) accomplished this for 2024-T4 aluminum by changing the strength coefficient and holding the strain hardening exponent constant. This same type of approach would probably work for any material which only softens or hardens. For a metal, such as mild steel, which hardens and softens, modeling would be more difficult.

The need to model the transients of hardening or softening would depend on the accuracy of the rest of the stress-strain model, i.e., if stable loop shape cannot be modeled with good accuracy, there is no need to include the transients. Unlike cyclic relaxation of mean stress, cyclic hardening or softening is only related to fatigue damage in an indirect manner.

Cyclic Relaxation of Mean Stress

An example of the cycle-dependent relaxation of mean stress is shown in Fig. 12. Being able to predict this type of relaxation for estimating fatigue lives of actual structures is particularly important when large residual stresses are induced by occasional overloads. At lower loads there may be enough plastic deformation at the critical location to cause cyclic relaxation. This situation could occur even if the majority of the structure is behaving elastically.

Not unlike cyclic hardening and softening, cyclic relaxation is difficult to mathematically characterize. As a testing problem, it is difficult to separate cyclic relaxation from hardening or softening. The presence or absence of a large mean stress at the critical location in a structure can potentially alter the life by a factor of a hundred or more. Thus, it is important to accurately model cyclic relaxation. Efforts to estimate cyclic relaxation rates have not been completely successful (31). Several methods have been used to simulate cyclic relaxation of mean stress (11, 29, 20), all of which are utilized in conjunction with a computer based model.

Models of Cyclic Stress-Strain Behavior

The ideal model of cyclic stress-strain response should be capable of generating individual stress-strain loops so as to simulate cyclic hardening or softening and cyclic relaxation of mean stress. Another characteristic of metals which must be modeled is the history dependence of the material. This is an essential characteristic to be simulated if random or block loading is present. Several models have been developed which account for memory (history dependence), cyclic hardening or softening, and cyclic relaxation of mean stress (11, 20, 32).

Martin, et al. (11) and Wetzel (20) simulate the stress-strain curve by small linear segments. Jhansale (32) utilizes smooth curves and programs the observed behavior, such as memory.

If fatigue damage is to be viewed as a continuous process, the amount of "bookkeeping" is very large. Models of stress-strain behavior which can be programmed for the digital computer are desirable. The mathematics of a model similar to that proposed by Martin, et al. (11) is described in detail in the Appendix. An example of this model's ability to simulate the initial cyclic stress-strain behavior of 2024-T4 aluminum is shown in Fig. 13.

A general stress-strain model that includes transients does not exist. Each model relies on empirical expressions for cyclic hardening or softening and relaxation. These expressions vary for each material. Conceivably enough simplifying assumptions could be made to derive a general model. If hardening or softening were considered to be a two-step process by which the material jumped from the monotonic to the stable cyclic stress-strain curve, a general model might be conceived. The model proposed by Martin, et al. (11) employed a relaxation expression which contained only one constant. This expression would certainly work for any material if the rate at which mean stress relaxed was not important. The model would need only six experimentally determined constants to simulate the stress-strain response of a metal. These are: elastic modulus, monotonic and stable cyclic strength coefficients and strain hardening exponents, and the mean stress relaxation constant.

The purpose of predicting stress-strain response is to determine the parameters necessary for making fatigue predictions. Such information as stress amplitude, mean stress, total strain, elastic strain, plastic strain, etc., are needed for each reversal or increment in the load history.

SMOOTH SPECIMEN FATIGUE BEHAVIOR

Axially loaded unnotched specimens with cylindrical or hourglass test sections can be subjected to completely reversed cycling between constant strain limits to determine the strain-life curve. Some metals undergo cycle-dependent hardening while others cyclically soften. The transient hardening or softening occurs rapidly at first then gradually slows until, at about half of the fatigue life, further change in the size and shape of the hysteresis loop is difficult to detect. The behavior can then be considered stable and a stable stress-strain hysteresis loop can be said to exist. The width of the loop at zero stress is the plastic strain range, $\Delta \epsilon_p$, and the height of the loop is the stress range, $\Delta\sigma$. Each time the direction of straining is reversed the initial unloading is elastic. The elastic modulus, E, does not change significantly during cyclic loading for most engineering metals.

Fatigue Properties

A log-log plot of strain range versus reversals to failure for most engineering metals will be similar to that shown in Fig. 14. At short lives the plastic strain range is large compared to the elastic strain range. At long lives the elastic strain is larger. There is a transition region where the elastic and plastic strain ranges are nearly the same. The fatigue life when they are equal is called the transition fatigue life, $2N_t$. A mathematical relationship for the strain-life curve may be obtained if the elastic and plastic components of the strain range are plotted separately as indicated in Fig. 14.

$$\frac{\Delta\epsilon}{2} = \frac{\Delta\epsilon_e}{2} + \frac{\Delta\epsilon_p}{2} = \frac{\sigma_f'}{E}(2N_f)^b + \epsilon_f'(2N_f)^c \qquad (6)$$

The constants b and σ_f'/E are the slope and intercept of the elastic strain versus life line, and ϵ_f' and c are similar constants for the plastic strain line. For a constant amplitude test the number of reversals to failure, $2N_f$, is equal to twice the number of cycles.

If sufficient fatigue data are not available to establish the fatigue properties (constants in Eq. 6) they can be estimated from tension properties. The fatigue strength coefficient σ_f' is nearly equal to the true fracture strength, σ_f, and the fatigue ductility coefficient, ϵ_f', is approximately equal to the true fracture ductility, ϵ_f. The fatigue ductility exponent, c, is usually a constant value of approximately -0.6 for most engineering metals. It is more difficult to estimate the value of the fatigue strength exponent, b. For wrought metals it can usually be shown that the fatigue strength at 10^6 reversals is approximately one half of the ultimate tensile strength, S_u. This estimate, coupled with the approximation that $\sigma_f' \approx \sigma_f$, gives an approximate value of b of $-1/6 \log (2\sigma_f/S_u)$.

The above approximations should be used only for preliminary analyses and with great caution. Actual fatigue test data such as shown for SAE 4340 steel in Figs. 15 through 20 should be used to determine the fatigue properties. The cost and time needed to generate such data can be justified by the fact that once the cyclic properties for a metal in a particular condition have been determined they can be used as a basis for fatigue damage analysis of a variety of components made of the metal subjected to virtually any history of loading.

More details on the cyclic behavior of metals are given elsewhere (3, 4, 7, 26, 28, 30). Procedures for approximating the cyclic stress-strain properties from various tests on a single specimen are described in the Appendix.

Effect of Cyclic Overstrain

If fatigue specimens are first overstrained a few cycles at a strain range between one and two percent (Fig. 18), the life will generally be shorter at intermediate and long lives than if no overstraining had been applied (14, 15). The magnitude of the initial cyclic overstraining does not seem to affect the resulting strain-life curve as long as it is large enough to cause cyclic plastic strain. For life calculations where overstrain may occur during component fabrication or at any time during service, the fatigue data should be determined from initially overstrained test specimens.

For some steels and possibly other metals the cyclic inelastic strains observed at intermediate and long lives are affected by occasional cycles of larger magnitude. Greater inelastic strains result for more frequently applied or larger overstrains (14). This effect eliminates the endurance limit for steel as shown in Fig. 19. In such cases where the stress-strain relationship is not unique, the use of a strain-life curve determined as described above is questionable. It must be decided whether total strain, plastic strain, or stress are more significant for calculating fatigue lives. The use of the plastic strain-life equation,

$$\frac{\Delta\epsilon_p}{2} = \epsilon_f' (2N_f)^c \qquad (7)$$

is supported by mechanistic arguments and by experimental evidence (14). It is recommended that the plastic strain versus life relationship at intermediate and long lives be determined from tests with periodic overstrains. If the inelastic strains that occur at long lives are too small to measure, a straight line extrapolation on the log-log plot of the shorter life inelastic strain versus life data should be made (see Fig. 15). Also, the cyclic stress-strain curve determined from an incremental step test may differ from that determined from constant amplitude tests (14). The lower curve should be used in fatigue analysis.

The implications of the detrimental influence of overstrain in the fatigue analysis of structures in service are obvious. Many components experience plastic strain during fabrication, or are overloaded in service, which is similar to an overstrain on a smooth specimen. Thus, it is appropriate to periodically overstrain all test samples used to establish base line fatigue properties for purposes of cumulative fatigue damage analysis.

Effect of Mean Stress

If a tensile mean or residual stress is present during fatigue, the life will be shorter than if it is not present. A compressive mean or residual stress will have the opposite effect. Fatigue life calculations at intermediate and long lives must include the effect of mean and residual stresses.

At short lives the plastic strains are sufficiently large to cause an accumulation of deformation if there is a mean stress. If a test is conducted in stress control, the mean strain will increase as the specimen is cycled. This behavior is called cycle-dependent creep. For strain controlled conditions the mean or residual stress will relax (5, 31) in a cycle-dependent manner if the inelastic strain is sufficiently large. Cycle-dependent relaxation of mean stress is illustrated in Fig. 12. If the inelastic strain range is of the same order or larger than the elastic strain range, no significant mean stress will exist after a few cycles (5). A mean stress can therefore be removed by strain cycling one or two cycles at a large strain range and then gradually reducing the strain range to zero. This technique is used after cyclic overstraining discussed above to insure that the specimen is returned to zero stress and strain before continuing the test at a small level of cyclic stress or strain, Fig. 18.

Several extensive studies of mean stress have been carried out for 2024-T4 aluminum and SAE 4340 steel (10, 13) as a part of this investigation. Wilson (13) generated data on 2024-T4 aluminum for constant mean stress and varying mean stress loading. Using the constant stress data, life estimations were made for the varying mean stress tests. Most of the life estimations over-estimated the life of the specimens. Topper and Sandor (10) later studied the effect of mean stress with constant amplitude data based on prestrained specimens. Tensile and compressive mean stress tests were performed on smooth specimens that were cyclically prestrained. They found the following equation to fit completely reversed and mean stress data reasonably well.

$$\frac{\Delta\epsilon_r}{2} = \frac{\Delta\epsilon}{2} + \frac{\sigma_o^{\alpha}}{E} \tag{8}$$

where $\Delta\epsilon_r/2$ is the "equivalent completely reversed strain amplitude." Equation 8 defines a fully reversed strain amplitude that would give the same life as a strain amplitude of $\Delta\epsilon/2$, coexisting with a mean stress, σ_o. The exponent, α, was reported as 0.73 for 2024-T4 aluminum and 0.89 for SAE 4340 steel. The correlation for the constant amplitude data, including that with mean stress, was good, Fig. 17.

Equation 8 also was used to estimate the fatigue lives of the varying mean stress data of Ref. (13). These life estimations were sufficiently accurate when prestrained data was used. Damage summations were from 0.55 to 1.3. Thus, some of the effects observed by Wilson (13) are believed to be due to the prestrain caused by imposing a mean stress.

Dowling (14, 15) studied the effect of mean stress on SAE 4340 steel and 2024-T4 aluminum. Various mean stress parameters were investigated. All specimens were initially overstrained and most of the steel specimens with lives longer than 10^5 cycles were periodically overstrained. Several mean stress parameters were considered for calculating an equivalent completely reversed amplitude of stress. Four of these parameters are listed below:

$$\sigma_r = \frac{\sigma_a}{1 - \sigma_o/S_u} \qquad \text{Smith (33)} \tag{9}$$

$$\sigma_r = \frac{\sigma_a}{1 - \sigma_o/\sigma_f} \qquad \text{Morrow (30)} \qquad (10)$$

$$\sigma_r = \sigma_a + \frac{\sigma_o}{d} \qquad \text{Stulen (34)} \qquad (11)$$

$$\sigma_r = [(\sigma_a + \sigma_o)(\sigma_a)]^{\frac{1}{2}} \qquad \text{Smith, et al., (35)} \qquad (12)$$

where S_u is the ultimate strength, σ_f is the true fracture strength and d is a constant for a particular material. Dowling reported that Eq. 11 gave the best agreement for both metals. Figure 20 shows the calculated values from Eqs. 11 and 12 plotted as σ_a/σ_r versus σ_o/σ_r.

In another investigation of this nature (36) the effect of prestrain and mean stress was studied for SAE 1015 steel. It was found that both Eqs. 10 and 12 agree reasonably well with the data.

The accurate fit of the mean stress data of Eqs. 8 and 11 is due to the constants which are determined from actual mean stress data. To utilize either of these equations, mean stress data must be generated. Equations 9 and 10 have monotonic tension properties as input. Equation 12 does not rely on any materials properties but relates directly to completely reversed fatigue data. The final choice of the mean stress parameter will depend on the data available. In most practical cases the mean stress present at the critical location in a part can not be very large because of the presence of cyclic plasticity. For this reason nearly any mean stress parameter is satisfactory since they do not deviate significantly from each other for small mean stresses.

FATIGUE DAMAGE ANALYSIS

Assuming that an accurate relation exists between nominal and local stress-strain behavior, that the stress-strain response of the metal can be simulated, and that appropriate smooth specimen fatigue data are available, a method of combining these elements into an efficient cumulative fatigue damage procedure is necessary. This procedure must be able to calculate and keep account of the many variables which occur in realistic loading situations. One such procedure which has been developed (11) is based on a model which is suitable for digital programming. Fatigue damage analysis of simple histories is possible without the aid of a computer but might be very time consuming. Tucker (18) used such a method wherein the monotonic and cyclic stress-strain curves were used to estimate mean stress and plastic strain for complicated, but short, loading spectra.

Fatigue Damage Criteria

By knowing the stress-strain response of the material at the critical location, fatigue estimates can be made by computing the damage from the fatigue properties of smooth specimens. Since at any time during a load spectrum the stress and strain at the critical location is known, a large amount of freedom is possible in selecting the fatigue damage criteria to be used.

Nearly every parameter imaginable has been used as a basis for summing fatigue damage. During the course of this investigation, cyclic strain modified to account for mean stress effects, was found to be the most convenient parameter for the type of problems analyzed. Strain is a particularly attractive basis for damage summations, since a log-log linear relation usually exists between plastic strain and life (37, 38) and elastic strain and life (39). Thus, a mathematical expression can be used for damage which is desirable if a computer based model is used. However, it is possible to store fatigue data in tabular form and interpolate for damage estimates.

Fatigue damage is summed on the above basis in the linear manner proposed by Palmgren (40) and Miner (41). Many of the errors which were once attributed to the method of summing damage using nominal stress-life relations have been since traced to other sources. Serious errors have been due to not properly accounting for mean stress and the effect of overstrain. For certain types of loading patterns, the way in which cycles are counted can also be important. The choice of a cycle counting method is particularly critical if the history involves occasional shifts in the mean strain that are large compared to the cyclic strain at each mean level. The ground-air-ground cycle in aircraft is an example.

Cycle Counting

Procedures for interpreting complex load, stress, or strain versus time histories are called cycle counting methods. A number of different cycle counting methods have been reviewed by Dowling (15). Only the range pair and the rain flow methods count strain cycles that correspond to closed stress-strain hysteresis loops. These two cycle counting methods are described and compared by Dowling (15).

The mean stress for each closed stress-strain hysteresis loop should be included in the damage analysis. The mean stress is simply the average of the maximum and minimum stresses occurring during the cycle. If strain-life curves for various values of mean stress are available, the life for any combination of strain range and mean stress can be found by interpolating between the curves. One of the mean stress parameters described in the last section can also be used to account for mean stress.

Each closed stress-strain hysteresis loop can be assumed to be equivalent to one cycle during a constant amplitude test. If linear accumulation of fatigue damage is assumed, then the fatigue damage for each closed hysteresis loop is equal to the reciprocal of the fatigue life for a constant amplitude test at the same strain range and mean stress.

If a similar damage calculation is made for each closed hysteresis loop, the results can be added to determine the total fatigue damage for one repetition of the history analyzed. Failure is expected when the strain history is repeated a sufficient number of times for the accumulated damage to reach unity.

Some Applications of the Fatigue Damage Analysis

Utilizing the rain flow cycle counting method, prestrained and mean stress data, Dowling predicted the fatigue lives of smooth 2024-T4 aluminum (15) and SAE 4340 steel (14) specimens subjected to a variety of complicated histories. The results of these predictions are shown in Figs. 21 and 22. For the 2024-T4 aluminum the stress-strain response was calculated by hand, and the effect of mean stress on damage was taken directly from plots for 2024-T4 aluminum. For the SAE 4340 steel, a computer program of the type used in Ref. (11) was employed to determine the stress-strain response. Mean stress effects were estimated by Eq. 11. These results show that with good stress-strain simulation, a proper method of accounting for mean stress and prestrain, and with a reasonable cycle counting technique, accurate fatigue predictions can be made for smooth specimens. Note in Fig. 22 the importance of using periodic overstrained life data rather than constant amplitude results.

Martin (11) used the computer based model of stress-strain behavior in conjunction with Neuber's rule to predict the fatigue lives of plates with a center hole. Some of the results are shown in Fig. 23.

Wetzel (20) also utilized a computer based model to estimate fatigue lives of notched plates. In his analysis, damage is summed over small segments of the computer based cyclic model. This procedure eliminates the need to count cycles but produces similar results as the rain flow method of counting. Although this method was easier to program than the rain flow counting method, it is convenient only if a computer based model is employed. Most of the applications of the proposed fatigue damage analysis have been for small laboratory specimens. As a more realistic example, this analysis has been used to estimate the fatigue lives of some built-up box beams which have been tested by the Navy.

Application to Navy Box Beams

As an illustrative problem, a computer based fatigue damage analysis was used to estimate the fatigue lives of some of the built-up box beams that have been fatigue tested by the Navy over the past several years (42-46). Fatigue lives were computed for the constant amplitude load and test spectrum B fatigue tests reported in Ref. (42). Additional life estimations were made for other constant load amplitude fatigue tests reported in Ref. (43).

The box beams are built-up structures. General design, fabrication techniques and materials are representative of components used in aircraft structures. Four metals were used in the beams. An aluminum alloy, 7075-T6, made up the top and bottom plates where failure occurred. The beams were tested in three point bending as described in Ref. (42).

A brief summary of the procedure used for the box beam life estimations is presented here. A more detailed explanation is given in the Appendix.

Cyclic stress-strain data consisted of the monotonic and cyclic steady state stress-strain curves. Cyclic hardening and cyclic relaxation of mean stress were simulated by the computer model in much the same manner as stated in Ref. (11). Damage was based on either elastic or plastic strain. Mean stress was accounted for by Eq. 10. Each reversal was individually counted. A more elaborate method of counting was not employed at the time, since a program was not available which could store the large amount of data used for the block loading spectra.

Figures 24 through 26 show the fatigue life estimations made by the computer based fatigue damage analysis for the constant amplitude tests. Agreement is good for most of the data. After the estimations had been made, it was found that the tests were at times shutdown. This releases the load to zero. Upon reloading, the mean stress would be altered from its previous value. In Ref. (47) an attempt is made to account for this by putting in occasional zero minimum loads which improved the life estimations.

The variation of K_f with life, which is reported in Ref. (43), would also contribute to the discrepancies between actual and estimated lives. The fatigue notch factor is usually determined from long life fatigue data. For this problem, K_f was estimated by first determining K_t, from published photoelastic results. This value was converted to K_f, by the highly stressed volume approach discussed in Ref. (16). Considering that no previous testing was necessary for the analysis, the results are quite encouraging.

Figure 27 shows fatigue life data and estimations for the beams subjected to test spectrum B of MIL-A-8866. For the zero margin of safety, a definite block size effect is evident in the tests. The estimated lives did not show the block size effect exhibited by the actual test data. This block size effect could, in part, be attributed to the cyclic relaxation of mean stress, which would be more probable for the longer block sizes.

CONCLUSIONS, LIMITATIONS AND FUTURE DIRECTIONS

A procedure for performing cumulative fatigue damage analyses has been outlined. Several examples are presented of the successful application of this analysis to estimate the fatigue life of various specimens and parts made from representative aircraft metals. Inputs to the analysis consist of a known load, nominal strain or local strain history, the geometry of the part including its notches and stress raiser, and mechanical properties of the material from which the part is made.

Cyclic History

Virtually any complex cyclic history can now be analyzed due to improved methods of cycle counting, better understanding of the effects of overstrain on the cyclic σ-ϵ and fatigue resistance of metals, and the use of computers to perform cycle to cycle analysis of local stress and strain and to sum damage.

Difficulties would be encountered in the fatigue analysis of parts that are loaded from more than one source, particularly if the loads are not in phase. This would cause cyclic changes in the direction of the maximum stress at the critical location and precludes the use of only uniaxial materials data in the analysis.

Material Properties

The material input consists of a set of monotonic and cyclic stress-strain properties and fatigue properties including the effects of overstrain and mean stress. Metals with a yield point may not have unique cyclic properties and so are somewhat more difficult to accurately analyze for fatigue purposes.

Cast metals or parts with large initial flaws (such as weldments) would also be difficult to analyze, since their cyclic deformation and fracture resistance cannot be related directly to their bulk behavior in a "smooth" specimen.

Part Geometry

The geometry of the member to be analyzed is the most limiting of the inputs to the analysis. Presently, only simply notched members that can be assumed to obey Neuber's rule can be treated without resorting to methods of experimental stress analysis. Also, the critical location must be subjected to essentially uniaxial cyclic stress since the present analysis does not treat multiaxial stress states. Research is needed on the fatigue behavior of metals under cyclic multiaxial and nonproportional stressing.

Fatigue Life

The output of the fatigue damage analysis is the life for the initiation of a crack of the same order of size as the smooth specimens used to determine the base line fatigue data. This is a serious limitation on the analysis since the size of this crack is arbitrary and many structures and parts satisfactorily perform in fatigue long after cracks have initiated. The analysis should be extended to treat fatigue crack propagation as a sequence of crack initiation events ahead of the crack.

Despite the limitation discussed above as well as other simplification such as ignoring time and temperature effects, corrosion, and so on, it is felt that the procedure outlined here can be helpful in estimating the useful fatigue life of simple metal parts. As methods are developed to treat more of the complexities of real parts under actual service environments, the analysis can be altered and expanded to provide more accurate and meaningful life predictions.

To extend the analysis to treat more complex geometries, a more generally applicable method for analytically relating nominal and local stresses and strains needs to be developed. Perhaps an extension of elasto-plastic finite element analysis to cyclic problems will be possible in the future.

APPENDIX

COMPUTER BASED FATIGUE LIFE PREDICTIONS FOR NAVY BOX BEAMS

by

J. F. Martin

INTRODUCTION

In the body of this report various alternative methods for predicting the lives of notched members are presented. This appendix uses some of these methods to predict the fatigue lives of built-up box beam structures. References 42 through 46 describe the box beams and the type of loading employed. Only constant amplitude loading and Flight Spectrum B were analyzed.

The box beam was chosen because of its resemblance to aircraft structures designed by the Navy and because of the large amount of data available. Available smooth specimen materials data and existing computer programs are used for making the fatigue life estimations.

Minimal specimen testing was considered important. These minimal data were used for determining both stress-strain behavior characteristics and fatigue resistance. Also, an effort was made to minimize the amount of computer time needed to make the life predictions.

GENERAL APPROACH

The approach taken to the box beam analysis can be broken into four steps:

(1) Calculate the nominal stresses near the critical location.

(2) Use an appropriate mechanics analysis to relate nominal stresses to the local stresses and strains at the critical location.

(3) Determine, from smooth specimens, the uniaxial stress-strain behavior and the fatigue resistance of the metal where the crack initiates.

(4) Incorporate the above into a procedure to perform the computations necessary for the large number of cycles involved.

The analysis was made using techniques that were appropriate for the available smooth specimen data or that could quickly be generated. All full scale fatigue tests on the box beams were performed by the Navy and NBS (42-46). The beam was subjected to three point bending. Simple beam theory was used to calculate the nominal stress near the critical location for a particular load. Materials properties and fatigue data were either taken from reports from this contract or generated specifically for this problem. Neuber's rule was used as one relation between the notch root stresses and strains and the nominal stresses. A computer program, similar to that described in Ref. 11, incorporated all the necessary data into a fatigue damage procedure for the box beam problem.

CALCULATION OF NOMINAL STRESSES

The box beam configuration and details are shown in Fig. 28. Failure was assumed to occur in the tension side at the center set of rivets. Nominal stresses, S, for the various load histories were reported in Refs. 42 and 43. These stresses were obtained from strain gage readings that were converted to stresses from the stress-strain curve of the 7075-T6 aluminum. The simple flexure formula, Eq. 13, produced stresses approximately ten percent higher than experimentally determined.

$$S = \frac{\text{Moment x Half Depth of Box Beam}}{\text{Moment of Inertia}} \tag{13}$$

For the fatigue analysis, only the experimentally determined nominal stresses were used.

MECHANICS ANALYSIS FOR RELATING NOMINAL STRESSES TO LOCAL STRESSES AND STRAINS

Equation 3 relates the product of the change in local stresses and strains to the change in nominal stresses. This equation is only valid when the nominal region responds elastically. The only constants involved are the elastic modulus and the fatigue notch factor, K_f.

Determination of K_f

The fatigue notch factor can be determined by comparing the stress-life data for the beam and smooth specimens. This comparison is usually done at long live and necessitates construction and testing of the structure. For this problem, K_f is determined by photoelastic and analytical means. By this technique, it would not have been necessary to fabricate and test the beam to determine K_f.

The value of the theoretical stress concentration factor, K_t, was taken from Ref. 48 where values of K_t are reported for flat plates with various arrangements of circular holes. The box beam did not have continuous array of holes as does the photoelastic model. Figure 29 shows the portion of the box beam under consideration. The b/a ratio for the photoelastic model was 0.63 as compared to 0.66 for the box beam. For a d/b ratio of 0.19, Ref. 48 reported a K_t of 2.9.

The fatigue notch factor, K_f, was determined by a highly stressed volume approach discussed in Ref. 8. For most metals, Eq. 14 was found to be accurate.

$$K_f = K_t \left(\frac{V_n}{V_u}\right)^{0.034} \tag{14}$$

where V_n and V_u are the highly stressed volumes of the notched and unnotched specimens, respectively. For axially loaded plates with shallow notches,

$$V_n \approx 0.018\, tr\sqrt{rb_n} \qquad (15)$$

Here, t is the thickness, r the notch radius, and b_n the notched minimum width. The notched minimum width for the box beam was taken to be the width of the shaded area shown in Fig. 29. The unnotched specimen volume was for a cylindrical $\frac{1}{4}$" diameter specimen with a straight section of 0.66". From this information the approximate value of K_f was calculated to be 2.4. This value is an intermediate value of the various estimations reported in Ref. 43.

Local Stress-Strain

Equations 3 and 13 establish a relation between an applied load range and the product of the local stress and strain range. The solution to Eq. 3 is not unique for a given nominal stress range, ΔS. Without the materials stress-strain response, an infinite number of solutions exist for the product $\Delta\sigma\,\Delta\epsilon$. One means of obtaining a complete solution would be to deform a uniaxial specimen in a manner so as to satisfy Eq. 3. The smooth specimen would supply the needed relation between stress and strain range. However, since a testing machine capable of controlling under these conditions was not available, an analytical procedure was employed. This procedure required knowledge of the stress-strain behavior and fatigue resistance of the 7075-T6 aluminum at the critical location.

UNIAXIAL STRESS-STRAIN AND FATIGUE DATA

In Ref. 3 the monotonic and cyclic stress-strain properties and fatigue data for 7075-T6 aluminum are reported. However, the majority of the data were for large to intermediate cyclic strains. It was estimated that most of the strain cycles experienced at the rivet hole would be below this range. Therefore, additional data were obtained at lower strain amplitudes. The stress-strain properties were determined from a single uniaxial specimen, subjected to the strain history shown in Fig. 30. From this test the monotonic and cyclic properties are characterized. Figure 31 shows the monotonic stress-strain curve up to a total strain of 0.015. The cyclic stress-strain curve was determined from the set of loops shown in Fig. 32. A log-log plot of these data is shown in Fig. 33.

Mean Stress Relaxation

Cyclic mean stress relaxation data were also produced from the single specimen test. Cyclic relaxation was observed during the strain limits with compressive mean strains. Some of the hysteresis loops were shown in Fig. 12. The assumption is made that mean stress relaxation can be isolated from cyclic hardening or softening. If a sample is cycled for a sufficient number of cycles, a stable condition is usually established in-so-far as hardening is concerned. However, by observing the initial set of hysteresis loops, Fig. 12, it can be seen that the lower loop tips do not change at the same rate as the positive peaks. Thus, hardening and relaxation of mean stress are occurring simultaneously. Figure 34 shows the rate of mean stress relaxation. These relaxation data were used for establishing the relaxation parameter in the model of cyclic stress-strain behavior.

Fatigue Resistance

The last portion of the single specimen test was under constant strain until final fracture. This was done to obtain one data point for a strain-life plot for cumulative damage analysis. Strain-life curves could have been approximated by the data from this single specimen, had a means been available for determining the slopes of the lines involved. This was not necessary since sufficient strain-life data were available.

Figure 35 shows strain-fatigue life data, which were taken from Refs. 3 and 17 and from tests conducted for this investigation. The strain-life data at small strain ranges without overstrain were quite scattered. However, the overstrain data had less scatter and enabled a better linear log-log fit for the overstrain and large strain range data.

All the overstrain data were generated specifically for this problem. It is speculated that the effect of overstrain on smooth specimens is similar to the effect of fabrication on structural components. For this reason, only the overstrain data were used at long lives for this analysis.

COMPUTER FATIGUE DAMAGE ANALYSIS

The information thus far gathered is combined and utilized to form a fatigue damage analysis which is suitable for the digital computer. The computer program for this analysis is similar to that outlined in Ref. 11. The major differences are in the damage summation and the type of cyclic hardening employed.

The computer based damage analysis consists of three sections: (1) the simulation of uniaxial cyclic stress-strain response, which includes cyclic hardening and cyclic relaxation of mean stress, (2) the controlling limits for the stress-strain model, Neuber control, and (3) damage summation. These three subdivisions form the complete fatigue damage analysis program.

Cyclic Stress-Strain Response

The basic form of the stress-strain simulation portion of the analysis follows the rules for a "series" rheological model. This model is shown in Fig. 36. Memory capabilities are an inherent feature of the model. Memory is an essential characteristic for simulating irregular load histories. The stress-strain curve is approximated by a series of linear segments. The slope of any one segment is determined by the stiffnesses of the springs, E_i^{σ}, of the elements which are active. Whether or not an element is active depends on the frictional slider yield stress, $\overline{\sigma}_i$, and the residual stress, σ_i, locked in the element due to previous loading. Elements are always activated in ascending order. The details of adjusting the constants for the model to simulate a particular stress-strain curve, and then utilizing the model to approximate that curve are discussed below.

Determination of σ_i and E_i: The yield stresses, σ_i, and the spring stiffnesses, E_i^{σ}, for N elements are chosen in such a manner as to approximate the smooth stress-strain curve described by Eq. 5. This is illustrated in Fig. 37. The number of elements, N, is chosen large enough to construct a hysteresis loop for any loading that might be encountered during the analysis.

The constants for simulating the stress-strain behavior of 7075-T6 aluminum were established by first setting the frictional slider stresses and then the spring stiffnesses. The superscript σ on E_i^{σ} signifies that each spring stiffness is stress dependent. These stress dependent spring stiffnesses are the means by which mean stress is relaxed. The smooth curve, which the model approximates, represents a stress-strain relation for a particular degree of hardness. Thus, hardening or softening is accomplished by determining a new stress-strain curve and adjusting the constants of the model to approximate it.

The first yield stress, which ends the first linear segment as shown in Fig. 37, is chosen as

$$\bar{\sigma}_2 = K^* (\epsilon_p)^{n^*} \tag{16}$$

where n^* is either the monotonic or cyclic strain hardening exponent. The remaining yield stresses are incremented by a predetermined amount. For this analysis, ϵ_p was assigned a value of 0.0001 and the yield stresses were incremented by 1 ksi.

Since the equation of the smooth curve is known and the frictional stresses have been determined, the slopes of each segment, E_i^*, can be calculated.

$$E_i^* = \frac{\delta \sigma_i^*}{\delta \epsilon_i^*}, \quad (i = 2, 3, \ldots, N) \tag{17}$$

For the first segment, the slope E_i^* is the elastic modulus. Already knowing the frictional stresses

$$\delta \sigma_i^* = \bar{\sigma}_{i+1} - \bar{\sigma}_i \tag{18}$$

The corresponding changes in strain are

$$\delta \epsilon_i^* = \frac{\delta \sigma_i^*}{E} + \left(\frac{\bar{\sigma}_{i+1}}{K^*}\right)^{1/n^*} - \left(\frac{\bar{\sigma}_i}{K^*}\right)^{1/n^*} \tag{19}$$

For this case K^* and n^* are either the monotonic or cyclic strength coefficient and strain hardening exponent, respectively.

The reciprocal of the slope of the i^{th} linear segment is the sum of the reciprocals of the stiffnesses of the elements that have been activated.

$$\frac{1}{E_i^*} = \frac{1}{E} + \frac{1}{E_2^{\sigma}} + \frac{1}{E_3^{\sigma}} + \ldots\ldots + \frac{1}{E_i^{\sigma}} \tag{20}$$

for $i = 2, 3, \ldots, N$.

To save computer time, the sum of the reciprocals of the slopes of elements are stored as a single number, $\Sigma 1/E_i^{\sigma}$. Equation 20 is rewritten as

$$\frac{1}{E_i^*} = \frac{1}{E} + \Sigma \frac{1}{E_i^{\sigma}} \tag{21}$$

The value of E_i^{σ} is not a constant, but is dependent on the stress level at which the element is being used. Equation 22 is the relation for E_i^{σ} chosen for this simulation

$$E_i^{\sigma} = E_i \, f(|\sigma|) \tag{22}$$

where E_i is a constant for a particular stress-strain curve and relaxing function, $f(|\sigma|)$. The value of $|\sigma|$ is calculated at the midpoint of each linear line segment. If $f(|\sigma|)$ is of a form that will reduce E_i^{σ} with increasing $|\sigma|$, the model will cyclically relax mean stress. Such a function is

$$f(|\sigma|) = 1 - \frac{|\sigma|}{M} \tag{23}$$

where M is the relaxing constant which is determined from empirical data and does not change during the simulation. Equation 23 is rewritten as

$$\frac{1}{E_i^*} = \frac{1}{E} + \frac{(\Sigma \, 1/E_i)}{f(|\sigma|)} \tag{24}$$

Once the values of E_i^* are determined from Eqs. 17 through 19, the constants for each spring, $\Sigma(1/E_i)$, are calculated from Eqs. 23 and 24. At this point the cyclic stress-strain behavior of the metal whose stress-strain curve is described by Eq. 5, could be simulated if a value for the relaxation constant, M, is known.

Cyclic relaxation is inherently associated with the spring stiffnesses. The relaxation constant is determined by trial and error to fit the available relaxation data. Cyclic hardening is accomplished by re-evaluating the constants of the parameters in the rheological model to fit a different stress-strain curve as described by Eq. 5. In determining the constants E_i and $\bar{\sigma}_i$, all calculations are made ignoring any residual stresses from previous reversals. In this case, hardening was accomplished in two steps. The monotonic stress-strain curve was used for the initial stress-strain path. Once a predetermined plastic strain, $\epsilon_p = 0.0001$, was exceeded for any one cycle, the stable cyclic stress-strain curve was used as a basis for constructing the frictional slider stresses, $\bar{\sigma}_i$, and the spring stiffnesses, E_i, as outlined before. This is represented in Fig. 38. It should be noted that the residual stresses of all the elements which were left from previous reversals are still locked in. Although the spring stiffnesses and frictional slider stresses are changed, the residual stresses remain until the element is activated again.

Simulating Stress-Strain Behavior with the Model: Once the parameters $\bar{\sigma}_i$ and E_i have been determined, the mathematical form of the rheological model may be used to approximate the cyclic stress-strain behavior of the metal for which the constants were derived. The model constructs each segment of a hysteresis loop by determining the stress, σ_i^*, at which the next element will be activated and calculating the slope of the curve from the spring stiffnesses of the elements that are activated. Elements are activated in ascending order.

At the beginning of each reversal, the last point of stress and strain from the previous reversal is set as σ_1^* and ϵ_1^*. The signs of the frictional stresses are set. If stress and strain are increasing, the values of $\bar{\sigma}_i$ are negative. For a reversal where the stress and strain values are decreasing, $\bar{\sigma}_i$ are positive. The values of the residual stresses set by all previous reversals are known.

Starting with subscript 2, the stresses for each increment are calculated from

$$\sigma_i^* = - \bar{\sigma}_{i+1} - \sigma_{i+1} \tag{25}$$

The change in stress for that increment is

$$\delta\sigma_i^* = \sigma_i^* - \sigma_i^* - 1 \tag{26}$$

For each segment, the reciprocal of slope is

$$\frac{1}{E_i^*} = \frac{1}{E} + (\Sigma \frac{1}{E_i}) \frac{1}{f(|\sigma|)} \tag{27}$$

The change in strain for each segment is

$$\delta\epsilon_i^* = E_i^* (\delta\sigma_i^*) \tag{28}$$

The total strain is

$$\epsilon_i^* = \epsilon_i^* - 1 + \delta\epsilon_i^* \tag{29}$$

Thus, the model reconstructs the stress-strain curve, including the effect of memory, by linear approximations.

For each segment, a check is made to determine if the limits have been exceeded. If the limits were exceeded, a linear interpolation is performed. For a final stress of σ_f^*, all residual stresses activated for the reversal are reset at

$$\sigma_i = - \sigma_f^* - \bar{\sigma}_i \tag{30}$$

The same procedure is followed for the next reversal, unless a plastic strain of 0.0001 was just exceeded for the first time. Exceeding this plastic strain limit signals the program to again calculate the constants for the model using the cyclic stress-strain curve. This same procedure is followed for each reversal.

At this point the model was programmed for the digital computer with strain as the controlling limits. The inputs to the program were the elastic modulus, monotonic and cyclic strength coefficients and strain hardening exponents, and the relaxing constant. Initially, a high value of $M = 10^4$ ksi, was used. The model was checked to insure it could reproduce the monotonic and steady state cyclic stress-strain behavior. To determine the relaxing constant, the program was run for the strain limits shown in Fig. 30 with various values of M. A sample of the actual data and simulation results are shown in Fig. 34. Only the data during which mean stress relaxation occurred were of interest. A relaxing constant of 3×10^3 ksi was chosen.

Neuber Control Limits: For each linear segment of the stress-strain curve produced by the model, a check is performed to determine if the desired limits have been exceeded. For the box beam analysis the controlling limits were imposed by Eq. 3 for a particular ΔS. In Ref. 42 ΔS from Eq. 13 is calculated and the values are tabulated. These values were input into the program. Each time the product of local stress and strain range for a particular nominal stress range was exceeded, a linear interpolation was performed to satisfy Eq. 3 and the stress-strain relation.

Cumulative Fatigue Damage Summation

Damage summation was accomplished by linearly summing damage for each reversal. The rain flow counting method was not employed, since the data for this report were generated before a suitable program was available. The damage summed for any one reversal was determined either by the elastic strain or the plastic strain-life curve from Fig. 35. The plastic strain-life curve was used if the plastic strain exceeded 0.0014. For smaller plastic strains, the elastic strain-life curve was used. The equations shown in Fig. 35 were programmed into the analysis.

Mean stress was accounted for by an equivalent completely reversed stress amplitude expressed by Eq. 10. For reversals with large plastic strains, mean stress was not accounted for.

A computer program was written as shown in the schematic in Fig. 39. This program was written to accommodate the large amount of input data for the various flight spectra which were simulated. With the materials stress-strain and fatigue data as input along with the loads, fatigue life estimations were made for the constant amplitude and Flight Spectrum B tests. The results of these estimations are shown in Figs. 24-27 and are discussed in the main text.

SUMMARY AND DISCUSSION

As an illustrative problem, specific procedures, which were discussed in the main body of this report, were applied to the box beam problem. The procedures selected were those which could most readily be utilized for this problem. The procedure used for this example can be discussed under the headings of the general outline presented earlier.

1) Determination of the nominal stresses near the critical location

Experimentally determined nominal stresses as a function of applied load were taken from Refs. 42 and 43.

2) Mechanics analysis for relating nominal and local stress-strain behavior

Neuber's rule was used to relate nominal and local stresses and strains. Photoelasticity data was used to determine a K_t for a structure similar to the top plate of the box beam. The highly stressed volume approach was used to estimate K_f from K_t.

3) Uniaxial stress-strain and fatigue behavior

Since the Neuber relation does not independently determine local stress and strain but only a relation involving the product of local stress and strain range, characterization of the stress-strain behavior of the metal at the critical location is necessary. Data were generated to establish the monotonic and stable cyclic stress-strain behavior and the cyclic relaxation characteristics.

To incorporate the metal's stress-strain properties into a cumulative damage procedure, the strain-life data shown in Fig. 35 were used. Only prestrain data were included in the analysis and the effect of mean stress was accounted for by Eq. 10.

4) Procedure for estimating the fatigue lives of the box beams

Neuber's rule and the computer based model of the metal's stress-strain behavior were combined to determine the stress-strain response at the critical location. The stress-strain model primarily follows the rule governing the rheological model shown in Fig. 36. The model's constants are initially set to simulate the monotonic stress-strain curve. Hardening is accomplished by changing the model's constants to fit the cyclic stress-strain curve. Cyclic relaxation of mean stress is accomplished by making the spring stiffnesses stress dependent. For each reversal, damage is summed based on the simulation results.

The results of the application of this analysis to the box beam are encouraging. Future applications would help determine the extent to which this type of procedure will produce satisfactory estimates of fatigue life.

REFERENCES

(Asterisk denotes papers produced as a part of this program.)

1.* R. M. Wetzel, "Smooth Specimen Simulation of Fatigue Behavior of Notches," Journal of Materials, Vol. 3, No. 3, September 1968, pp. 646-657. See also: R. M. Wetzel, "Smooth Specimen Simulation of Fatigue Behavior of Notches," T. & A. M. Report No. 295, Department of Theoretical and Applied Mechanics, University of Illinois, Urbana, May 1967.

2.* R. M. Wetzel, JoDean Morrow, and T. H. Topper, "Fatigue of Notched Parts with Emphasis on Local Stresses and Strains," Naval Air Development Center Report No. NADC-ST-6818, September 1968.

3.* T. Endo and JoDean Morrow, "Cyclic Stress-Strain and Fatigue Behavior of Representative Aircraft Metals," Journal of Materials, Vol. 4, March 1969, pp. 159-175. See also: T. Endo and JoDean Morrow, "Monotonic and Completely Reversed Cyclic Stress-Strain and Fatigue Behavior of Representative Aircraft Metals," Aeronautical Structures Laboratory Report No. NAEC-ASL-1105, June 1966.

4.* R. W. Landgraf, JoDean Morrow, and T. Endo, "Determination of the Cyclic Stress-Strain Curve," Journal of Materials, Vol. 4, No. 1, March 1969, pp. 176-188.

5.* T. H. Topper, B. I. Sandor, and JoDean Morrow, "Cumulative Fatigue Damage under Cyclic Strain Control," Journal of Materials, Vol. 4, No. 1, March 1969, pp. 189-199. See also: T. H. Topper, B. I. Sandor and JoDean Morrow, "Cumulative Fatigue Damage under Cyclic Strain Control," Aeronautical Structures Laboratory Report No. NAEC-ASL-1115, June 1967.

6.* T. H. Topper, R. M. Wetzel, and JoDean Morrow, "Neuber's Rule Applied to Fatigue of Notched Specimens," Journal of Materials, Vol. 4, No. 1, March 1969, pp. 200-209. See also: T. H. Topper, R. M. Wetzel, J. Morrow, "Neuber's Rule Applied to Fatigue of Notched Specimens," Aeronautical Structures Laboratory Report No. NAEC-ASL-1114, June 1967.

7.* D. T. Raske and JoDean Morrow, "Mechanics of Materials in Low Cycle Fatigue Testing," Manual on Low Cycle Fatigue Testing, ASTM STP 465, American Society for Testing and Materials, 1969, pp. 1-25. See also: D. T. Raske and JoDean Morrow, "Appendix A - Low Cycle Fatigue Testing from the Mechanics of Materials Viewpoint," Appendix to Naval Air Development Center Report No. NADC-ST-6818, September 1968, pp. 39-71.

8.* T. H. Topper and JoDean Morrow, Editors, "Simulation of the Fatigue Behavior at the Notch Root in Spectrum Loaded Notched Members (U)," T. & A. M. Report No. 333, Department of Theoretical and Applied Mechanics, University of Illinois, Urbana, January 1970 (Final Report for Aero Structures Department, Naval Air Development Center).

9.* JoDean Morrow, R. M. Wetzel, and T. H. Topper, "Laboratory Simulation of Structural Fatigue Behavior," Effect of Environment and Complex Load History on Fatigue Life, ASTM STP 462, American Society for Testing and Materials, 1970, pp. 74-91. See also Ref. (2).

10.* T. H. Topper and B. I. Sandor, "Effects of Mean Stress and Prestrain on Fatigue Damage Summation," Effects of Environment and Complex Load History on Fatigue Life, ASTM STP 462, American Society for Testing and Materials, 1970, pp. 93-104. See also: T. H. Topper and B. I. Sandor, "Effects of Mean Stress on Fatigue Damage Summation," T. & A. M. Report No. 318, Department of Theoretical and Applied Mechanics, University of Illinois, Urbana, August 1968. See also Chapter III of Ref. (8).

11.* J. F. Martin, T. H. Topper, and G. M. Sinclair, "Computer Based Simulation of Cyclic Stress-Strain Behavior with Applications to Fatigue," Materials Research and Standards, Vol. 11, No. 2, February 1971, p. 23. See also: J. F. Martin, T. H. Topper, and G. M. Sinclair, "Computer Based Simulation of Cyclic Stress-Strain Behavior," T. & A. M. Report No. 326, Department of Theoretical and Applied Mechanics, University of Illinois, Urbana, July 1969. See also Chapter V of Ref. (8).

12.* S. J. Stadnick and JoDean Morrow, "Techniques for Smooth Specimen Simulation of the Fatigue Behavior of Notched Members," Testing for Prediction of Material Performance in Structures and Components, ASTM STP 515, American Society for Testing and Materials, 1972, pp. 229-252. See also: S. J. Stadnick, "Simulation of Overload Effects in Fatigue Based on Neuber's Analysis," T. & A. M. Report No. 325, Department of Theoretical and Applied Mechanics, University of Illinois, Urbana, 1969. See also Chapter IV of Ref. (8).

13.* R. B. Wilson, "Influence of Variable Mean Stress on Fatigue Damage," T. & A. M. Report No. 672, Department of Theoretical and Applied Mechanics, University of Illinois, Urbana, June 1967. See also: R. B. Wilson, "Influence of Variable Mean Stress on Fatigue Damage," M.S. Thesis, Department of Theoretical and Applied Mechanics, University of Illinois, Urbana, 1967.

14.* N. E. Dowling, "Fatigue Life and Inelastic Strain Response under Complex Histories for an Alloy Steel," T. & A. M. Report No. 354, Department of Theoretical and Applied Mechanics, University of Illinois, Urbana, April 1972. See also: Journal of Testing and Evaluation, Vol. 1, No. 4, July 1973, pp. 271-287.

15.* N. E. Dowling, "Fatigue Failure Predictions for Complicated Stress-Strain Histories," Journal of Materials, Vol. 7, No. 1, March 1972, pp. 71-87. See also: N. E. Dowling, "Fatigue Failure Predictions for Complicated Stress-Strain Histories," T. & A. M. Report No. 337, Department of Theoretical and Applied Mechanics, University of Illinois, Urbana, January 1971.

16.* D. T. Raske, "The Variation of the Fatigue Notch Factor with Life," M.S. Thesis, Department of Theoretical and Applied Mechanics, University of Illinois, Urbana, 1971. See also Chapter II of Ref. (8).

17.* D. T. Raske, "Section and Notch Size Effects in Fatigue," T. & A. M. Report No. 360, Department of Theoretical and Applied Mechanics, University of Illinois, Urbana, August 1972.

18.* L. E. Tucker, "A Procedure for Designing against Fatigue Failure of Notched Parts," Preprint of Society of Automotive Engineers, from Automotive Engineering Congress, Detroit, Michigan, January 10-14, 1972. See also: L. E. Tucker, "A Procedure for Designing against Fatigue Failure of Notched Parts," M.S. Thesis, Department of Theoretical and Applied Mechanics, University of Illinois, Urbana, 1970.

19. H. Neuber, "Theory of Stress Concentration for Shear-Strained Prismatical Bodies with Arbitrary Nonlinear Stress-Strain Law," Transactions, American Society of Mechanical Engineers, Journal of Applied Mechanics, Vol. 8, December 1961, pp. 544-550.

20. R. M. Wetzel, "A Method of Fatigue Damage Analysis," Technical Report No. SR 71-107, Scientific Research Staff, Ford Motor Company, August 1971. See also: R. M. Wetzel, "A Method of Fatigue Damage Analysis," Ph.D. Thesis, Department of Civil Engineering, University of Waterloo, Waterloo, Ontario, September, 1971.

21. C. R. Smith, "Small Specimen Data for Predicting Life of Full-Scale Structures," Fatigue Tests of Aircraft Structures: Low-Cycle, Full-Scale, and Helicopters, ASTM STP 338, American Society for Testing and Materials, 1962, pp. 241-250.

22. E. Z. Stowell, "Stress and Strain Concentration at a Circular Hole in an Infinite Plate," NACA TN 2073, 1950.

23. J. Schijve, "The Accumulation of Fatigue Damage in Aircraft Materials and Structures," AGARD-AG-157, Advisory Group for Aerospace Research & Development, North Atlantic Treaty Organization, January 1972.

24. J. H. Crews, Jr. and H. F. Hardrath, "A Study of Cyclic Plastic Stresses at a Notch Root," Experimental Mechanics, Vol. 6, No. 6, June 1966, pp. 313-320.

25. S. S. Manson and M. H. Hirschberg, "Crack Initiation and Propagation in Notched Fatigue Specimens," Proceedings of the First International Conference on Fracture, The Japanese Society for Strength and Fracture of Materials, Vol. 1, Sendai, Japan, September 1965, pp. 479-498.

26. R. W. Landgraf, "The Resistance of Metals to Cyclic Deformation," Achievement of High Fatigue Resistance in Metals and Alloys, ASTM STP 467, American Society for Testing and Materials, 1970, pp. 3-36.

27. P. C. Rosenberger, "Fatigue Behavior of Smooth and Notched Specimens of Man-Ten Steel, M.S. Thesis, Department of Theoretical and Applied Mechanics, University of Illinois, Urbana, 1968.

28. JoDean Morrow, "Cyclic Plastic Strain Energy and Fatigue of Metals," Internal Friction, Damping, and Cyclic Plasticity, ASTM STP 378, American Society for Testing and Materials, 1965, pp. 45-87.

29. H. R. Jhansale and T. H. Topper, "Cyclic Deformation and Fatigue Behavior of Axial and Flexural Members - A Method of Simulation and Correlation," Proceedings of the First International Conference on Structural Mechanics in Reactor Technology, Berlin, Germany, September 1972, Vol. 6, Part L, pp. 433-455.

30. JoDean Morrow, "Fatigue Properties of Metals," Section 3.2 of Fatigue Design Handbook, Society of Automotive Engineers, 1968.

31. JoDean Morrow and G. M. Sinclair, "Cycle-Dependent Stress Relaxation," Symposium on Basic Mechanisms of Fatigue, ASTM STP 237, American Society for Testing and Materials, 1958, pp. 83-109.

32. H. R. Jhansale, "Inelastic Deformation and Fatigue Response of Spectrum Loaded Strain Controlled Axial and Flexural Members," Ph. D. Thesis, Department of Civil Engineering, University of Waterloo, Waterloo, Ontario, Canada, March 1971.

33. J. O. Smith, "The Effect of Range of Stress on the Fatigue Strength of Metals," Bulletin No. 334, University of Illinois, Engineering Experiment Station, Urbana, February 1942.

34. F. L. Stulen, "Fatigue Life Data Displayed by a Single Quantity Relating Alternating and Mean Stress," AFML TR 65-121, Air Force Materials Lab., Wright-Patterson AFB, Ohio, July 1965.

35. K. N. Smith, P. Watson, and T. H. Topper, "A Stress-Strain Function for the Fatigue of Metals," Journal of Materials, Vol. 5, No. 4, December 1970, pp. 767-776.

36. P. Watson and T. H. Topper, "Fatigue Damage Evaluation for Mild Steel Incorporating Mean Stress and Overload Effects," Experimental Mechanics, Vol. 12, No. 1, January 1972.

37. L. F. Coffin, Jr., "A Study of the Effects of Cyclic Thermal Stresses on a Ductile Metal," Transactions, American Society of Mechanical Engineers, Vol. 76, August 1954, pp. 931-950.

38. S. S. Manson, "Behavior of Materials under Conditions of Thermal Stress," Heat Transfer Symposium, University of Michigan Engineering Research Inst., 1953, pp. 9-75. See also: NACA TN 2933, 1953.

39. O. H. Basquin, "The Exponential Law of Endurance Tests," Proceedings, American Society of Testing and Materials, Vol. 10, Part II, 1910, pp. 625-630.

40. A. Palmgren, "Die Lebensdauer von Kugellagern," Zeitschrift des Vereines Deutscher Ingenieure, Vol. 68, No. 14, April 1924, pp. 339-341.

41. M. A. Miner, "Cumulative Damage in Fatigue," Transactions, American Society of Mechanical Engineers, Vol. 67, 1945, p. A159.

42. W. Breyan, "Effects of Spectrum Block Size and Stress Level on Fatigue Characteristics of Aluminum Alloy Box Beams under Fixed-Sequence Unidirectional Loading," Report No. NADC-ST-6811, Naval Air Development Center, Johnsville, Pennsylvania, September 1968.

43. W. Breyan, "Constant-Load-Amplitude Fatigue Characteristics of Aluminum Alloy Box Beams under Partially Reversed Loading," Report No. NADC-ST-7011, Naval Air Development Center, Warminster, Pennsylvania, October 1970.

44. W. Breyan and E. P. Roeser, "Effects of Spectrum Block Size and Stress Level on Fatigue Characteristics of Aluminum Alloy Box Beams under Random-Sequence Unidirectional Loading," Report No. NADC-ST-7013, Naval Air Development Center, Warminster, Pennsylvania, December 1971.

45. W. Breyan, "Summary of Test Results for Aluminum Alloy Box Beam Fatigue Program, Test Phases I-IV," Report No. NADC-72056-VT, Naval Air Development Center, Warminster, Pennsylvania, June 1972.

46. W. Breyan, "Effects of Block Size, Stress Level, and Loading Sequence on Fatigue Characteristics of Aluminum-Alloy Box Beams," Effects of Environment and Complex Load History on Fatigue Life, ASTM STP 462, American Society for Testing and Materials, 1970, pp. 127-166.

47. L. F. Impellizzeri, "Cumulative Damage Analysis in Structural Fatigue," Effects of Environment and Complex Load History on Fatigue Life, ASTM STP 462, American Society for Testing and Materials, 1970, pp. 40-68.

48. J. W. Dally and A. J. Durelli, "Stresses in Perforated Panels," Product Engineering, Vol. 27, No. 3, March 1956, pp. 188-191.

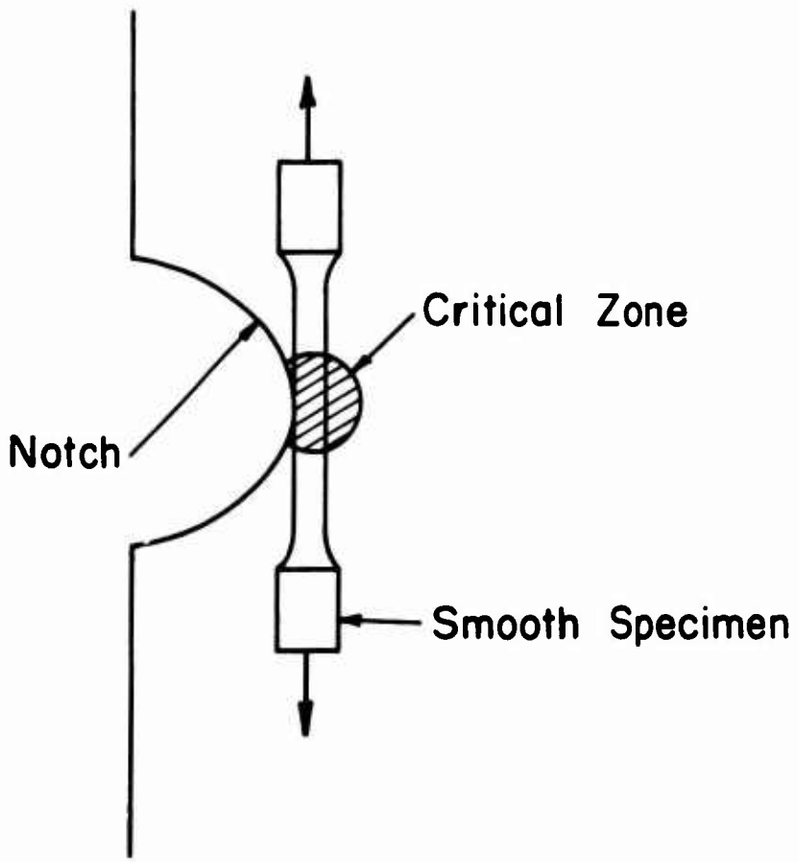

Fig. 1 Smooth Specimen Representation of Material at the Critical Zone

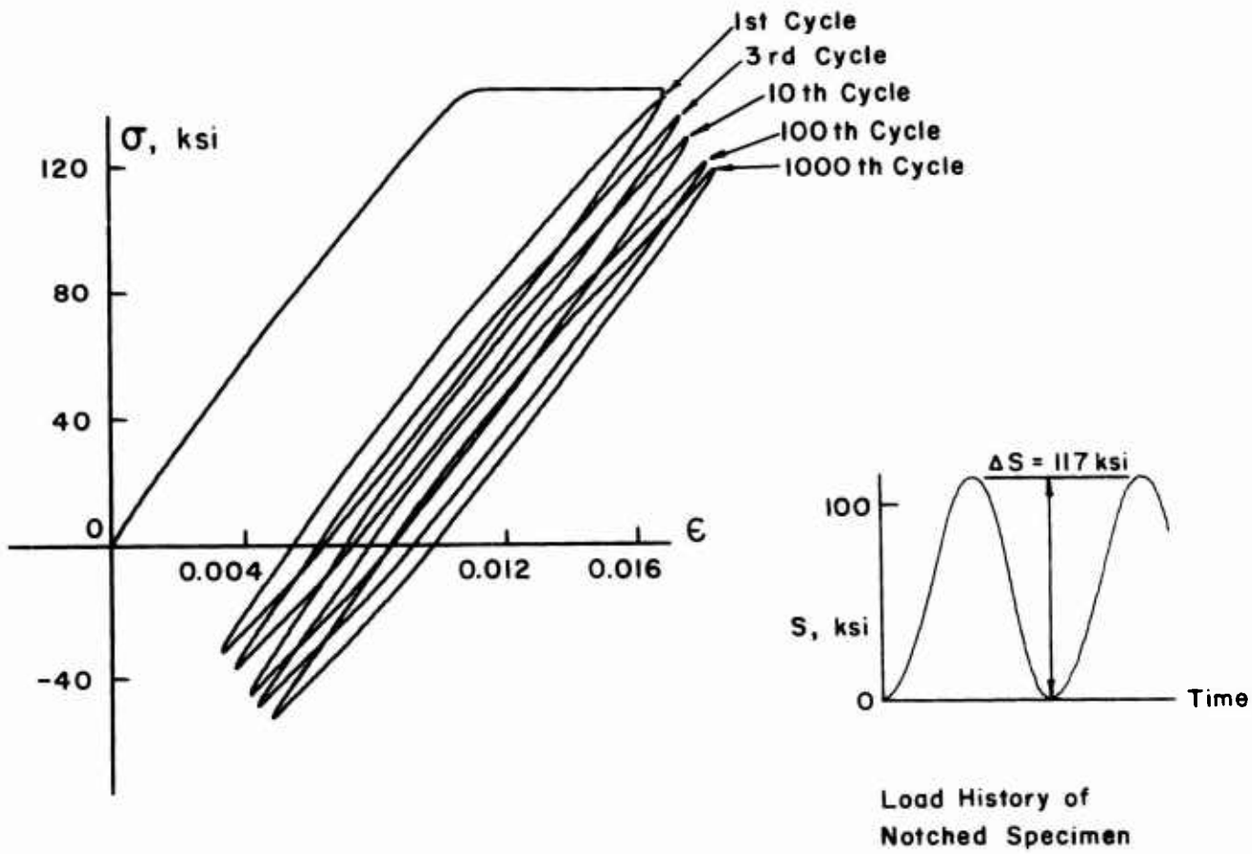

Fig. 2 Cyclic Softening and Relaxation of Mean Stress under Neuber Control (Ti-8Al-1Mo-1V, $K_f = 1.75$), (12)

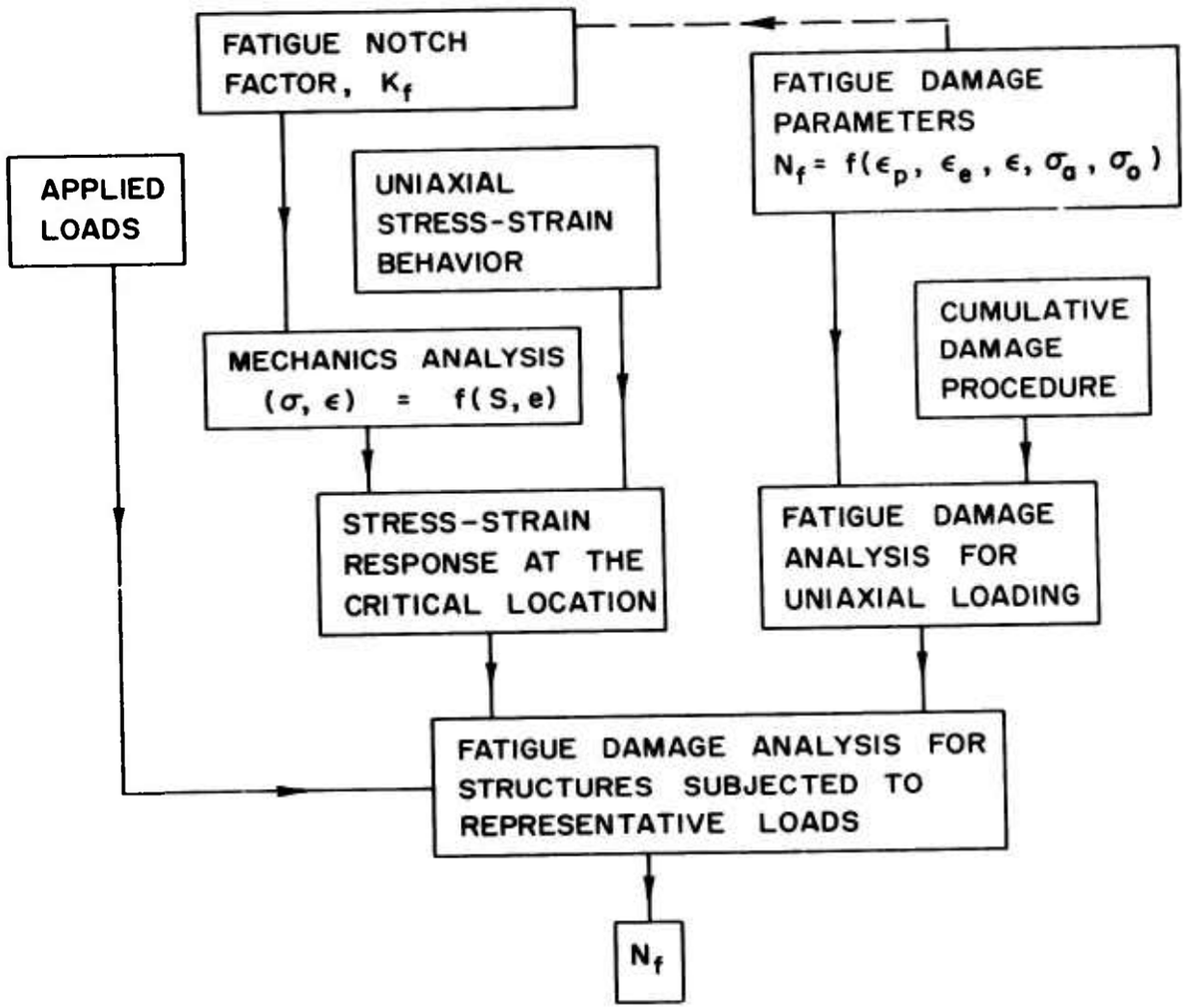

Fig. 3 Cumulative Fatigue Damage Procedure

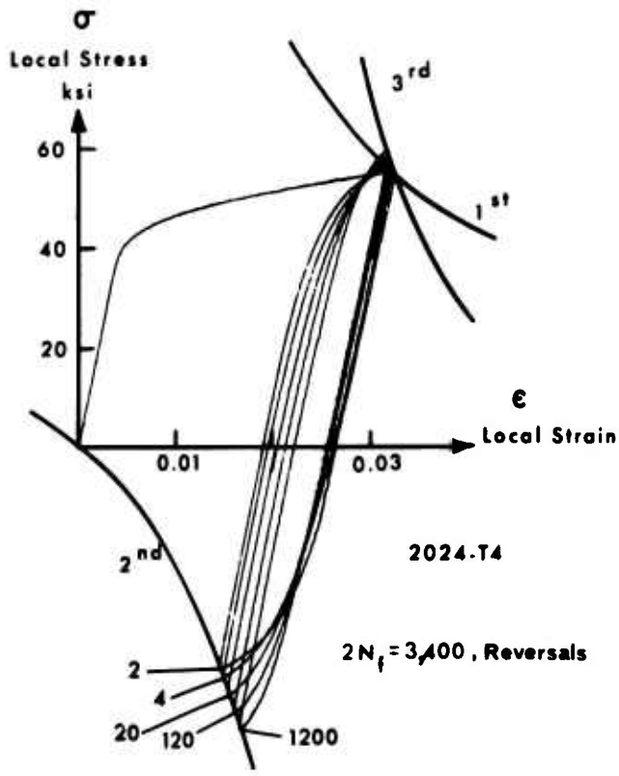

Fig. 4 Recorded Data from a Smooth Specimen Simulation of the Local Stress-Strain Behavior of a Notch, (1)

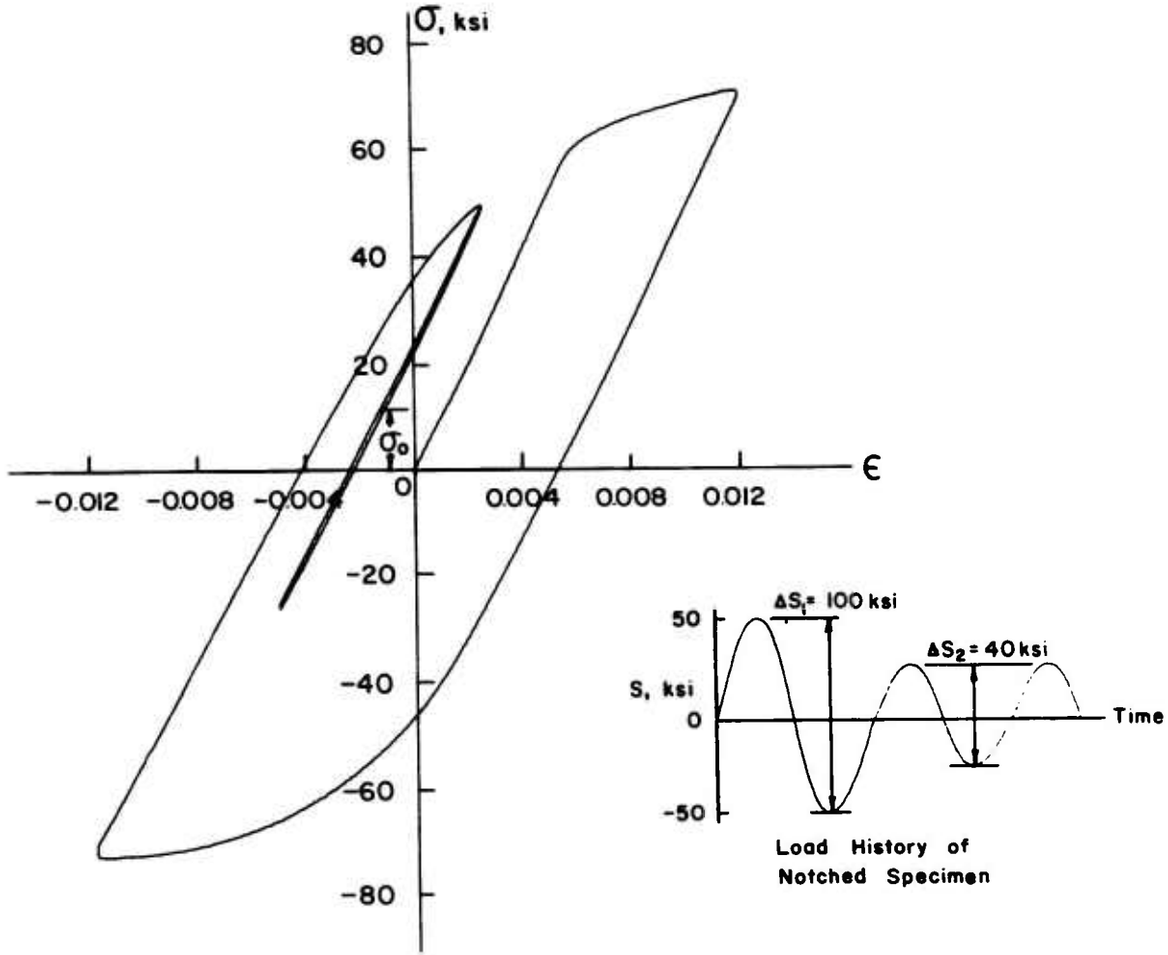

Fig. 5 Stress-Strain Response of a Smooth Specimen Notch Root Simulation (7075-T6 Aluminum, $K_f = 1.95$), (12)

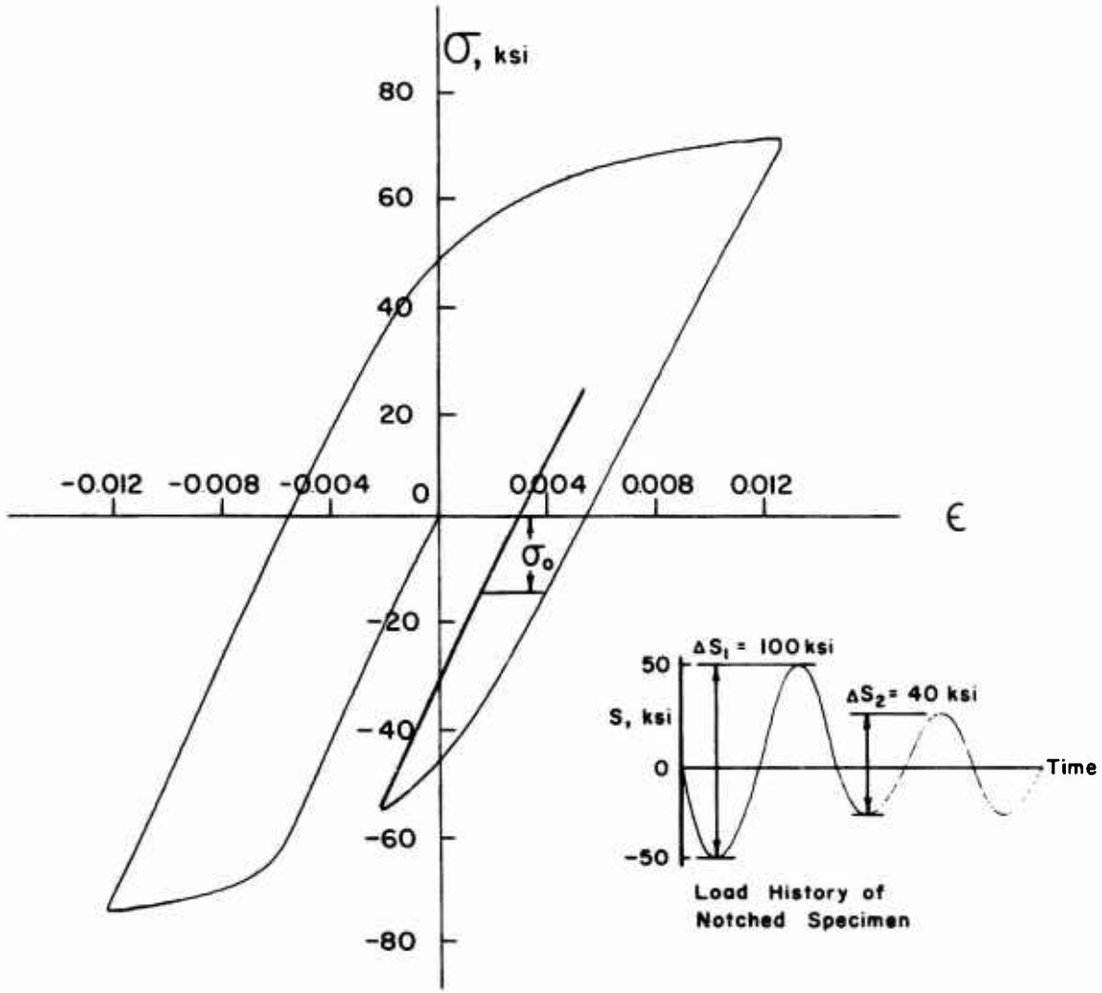

Fig. 6 Stress-Strain Response of a Smooth Specimen Notch Root Simulation (7075-T6 Aluminum, $K_f = 1.95$), (12)

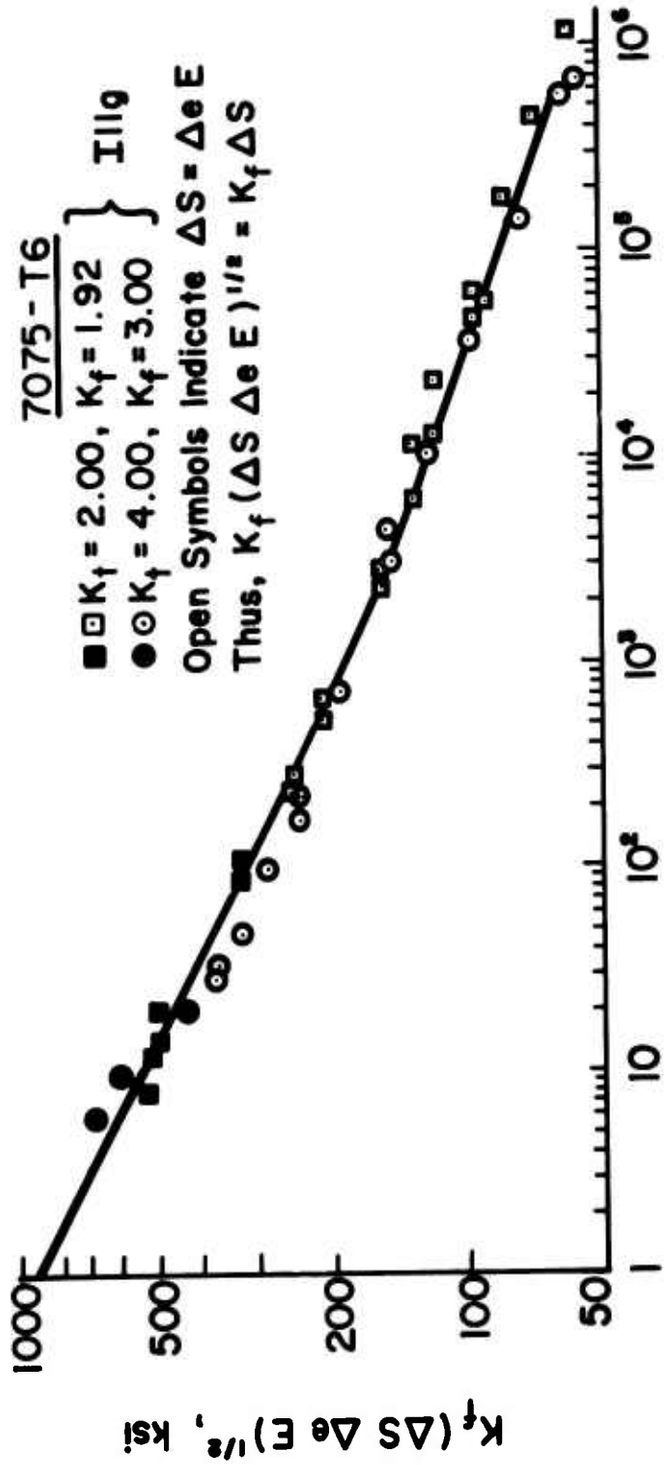

Fig. 7 Comparison of Notched Fatigue Data with Life Curves Predicted from Smooth Specimen Data (6)

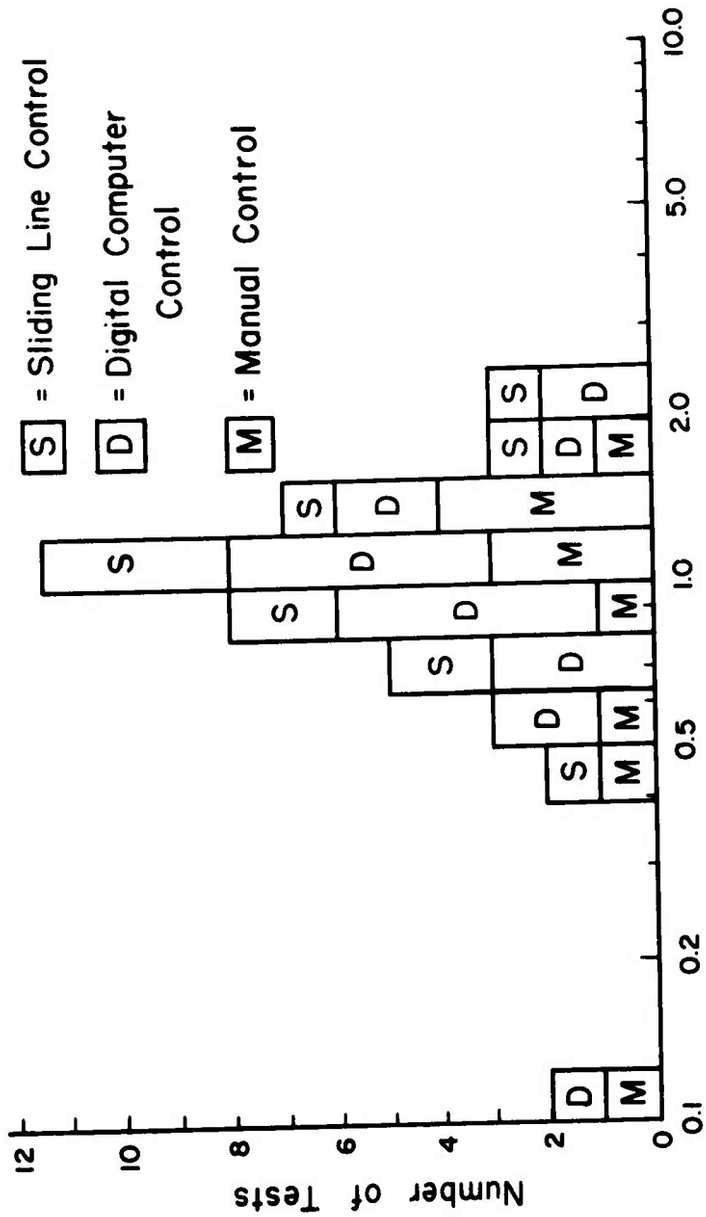

Fig. 8 Distribution of Failure Predictions (12)

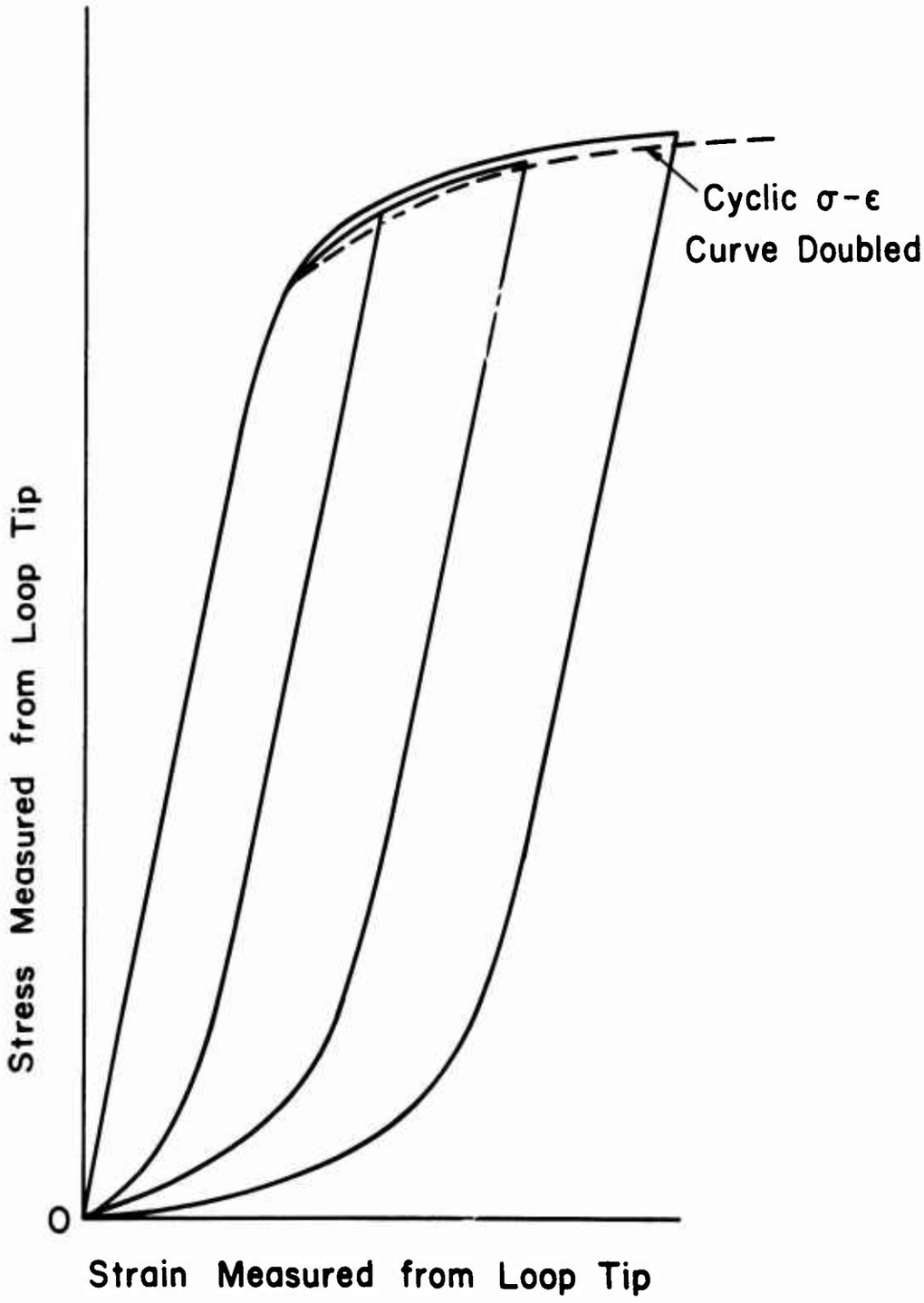

Fig. 9 Stress-Strain Response for 2024-T4 Aluminum (11)

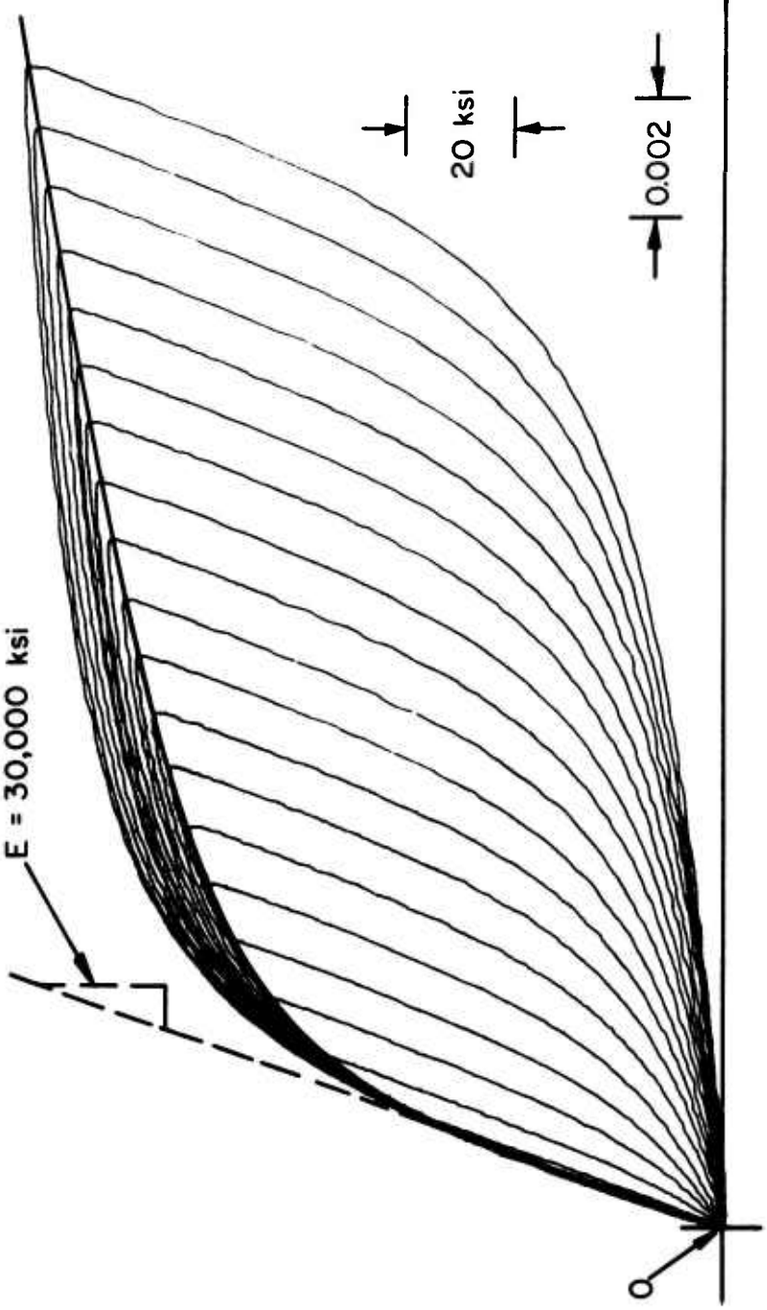

Fig. 10 Hysteresis Loops at Varying Strain Amplitudes for Man-Ten Steel(27)

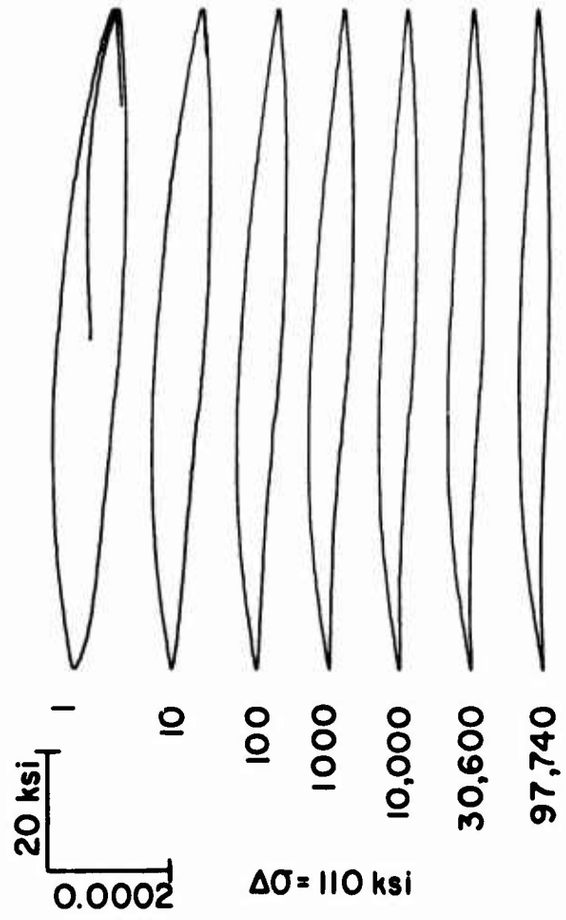

Fig. 11 Typical Stress–Inelastic Strain Hysteresis Loops during a Test with Overstrains every 10^5 Cycles for SAE 4340 Steel (14)

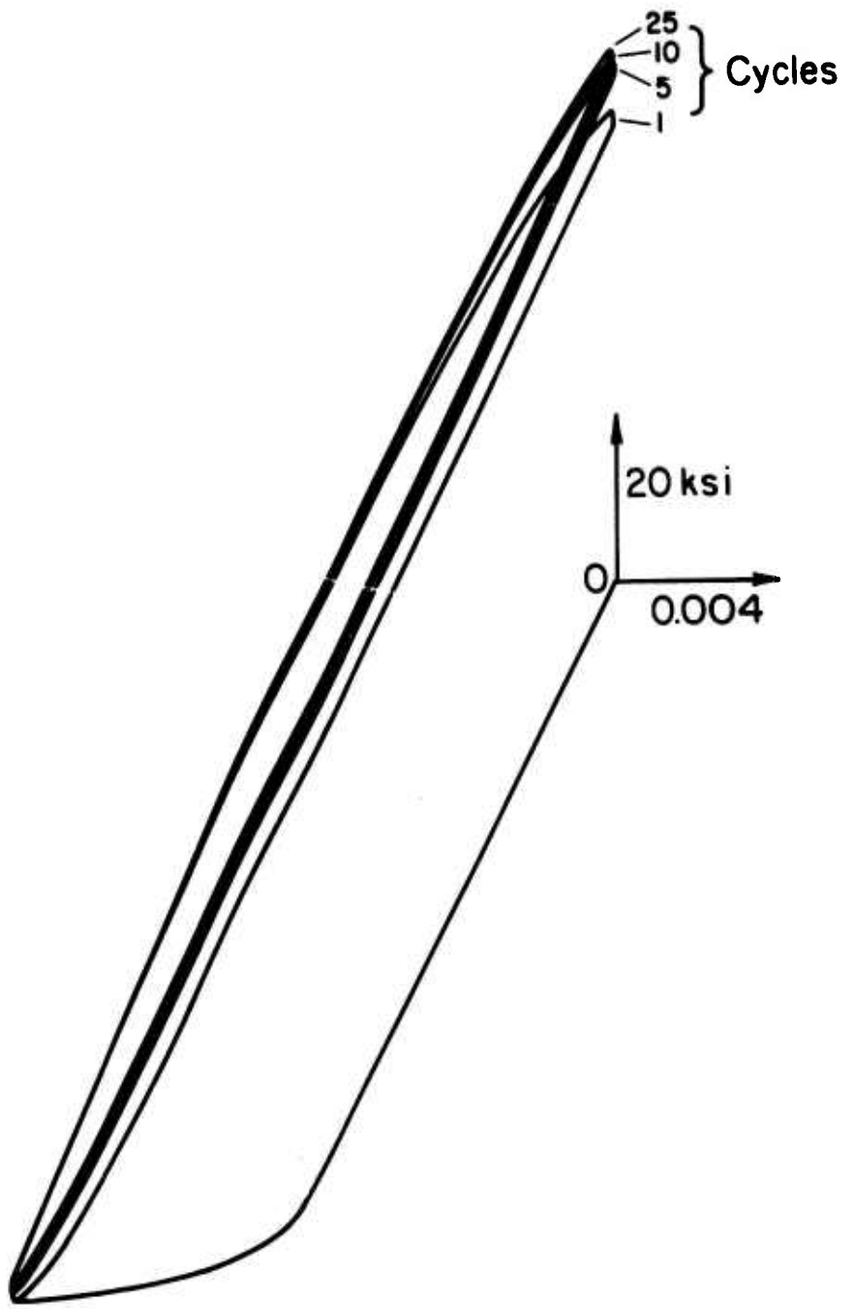

Fig. 12 Cyclic Relaxation of Mean Stress for 7075-T6 Aluminum

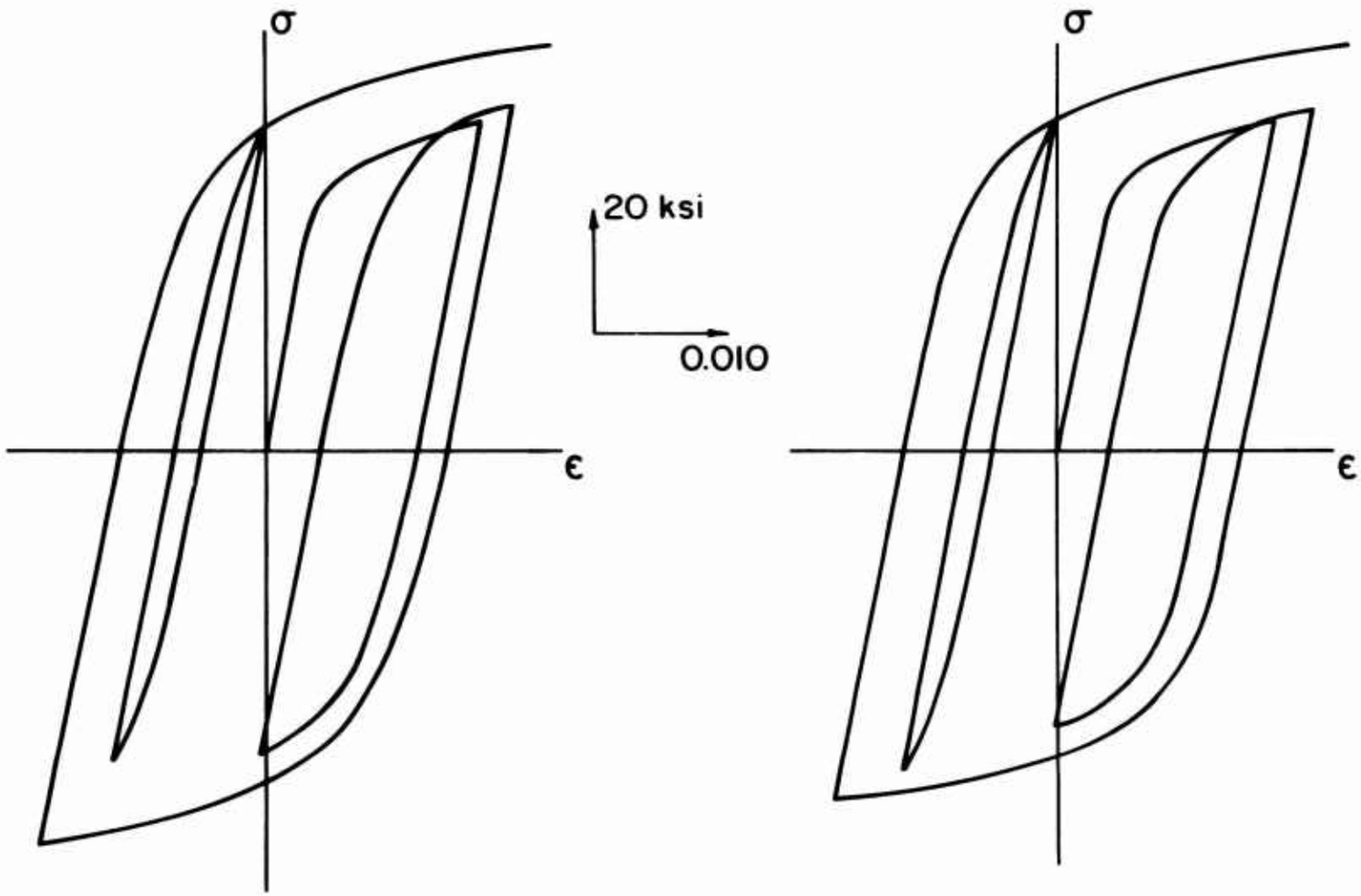

(a) Test Results (b) Simulation

Fig. 13 Actual and Simulated Stress-Strain Response of 2024-T4 Aluminum (11)

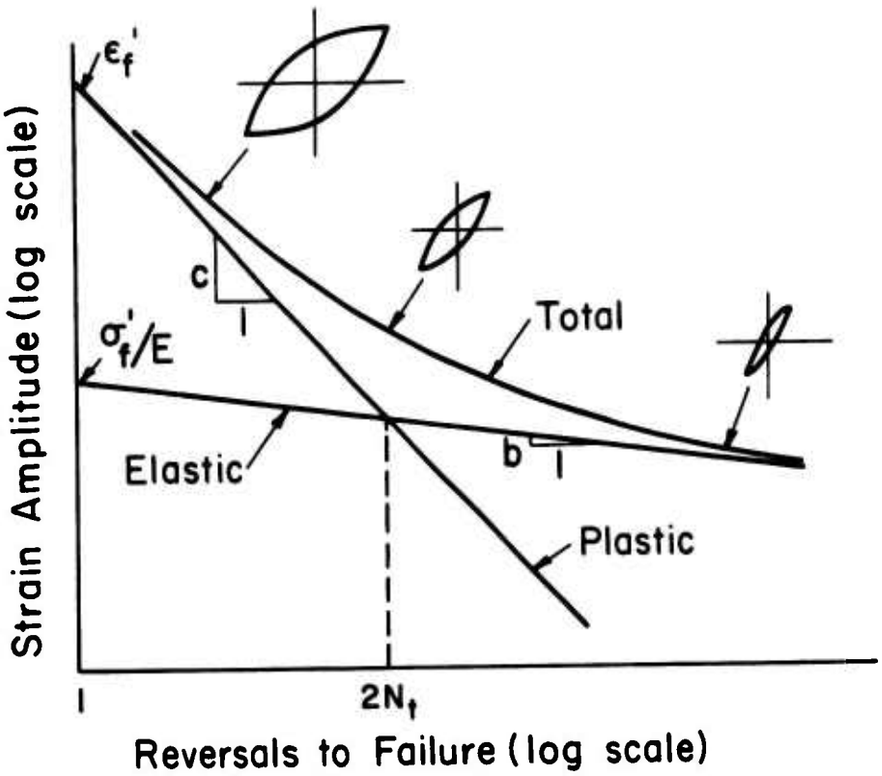

Fig. 14 Representation of Elastic, Plastic and Total Strain Amplitude–Fatigue Life Relations

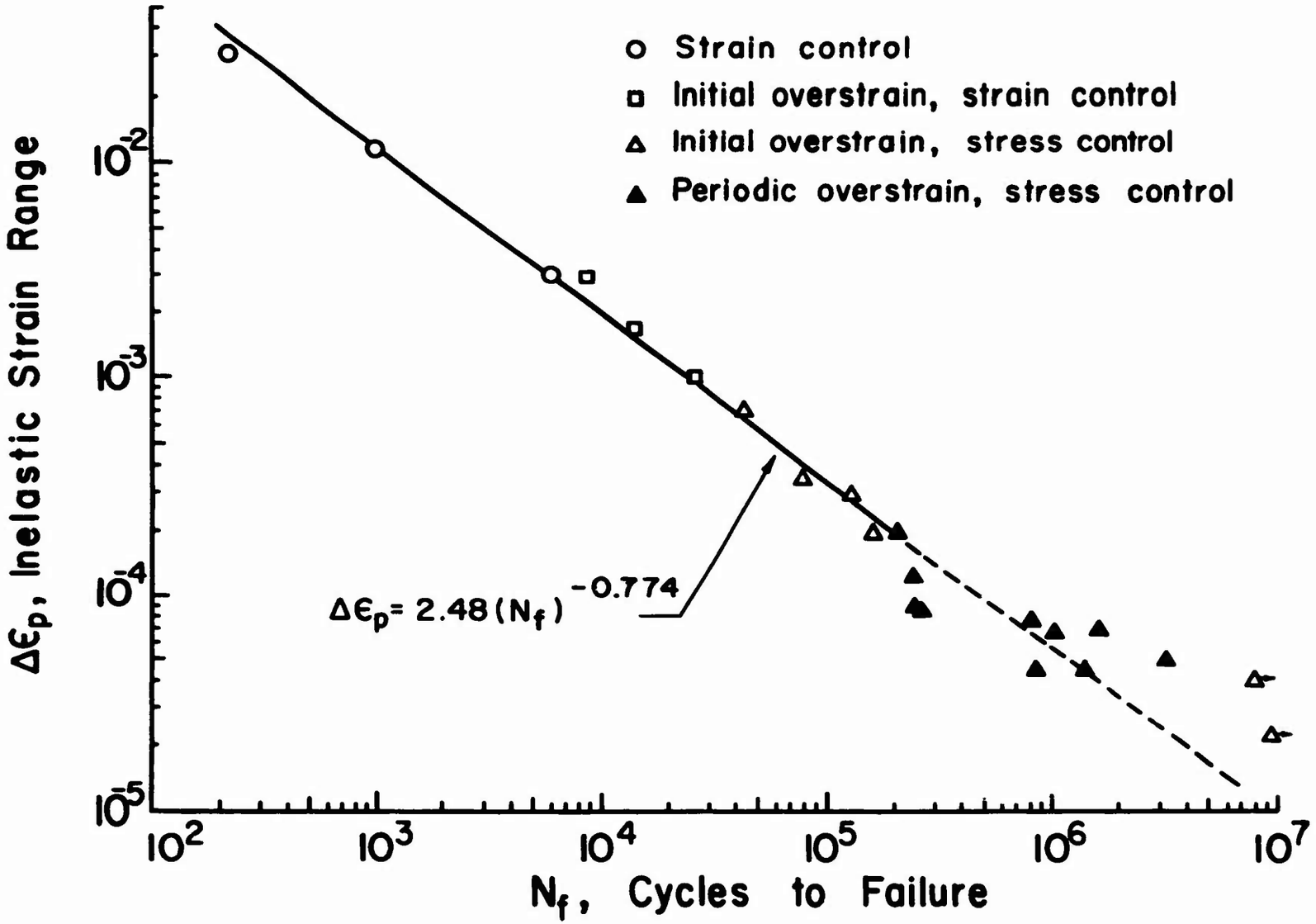

Fig. 15 Inelastic Strain versus Life for SAE 4340 Steel (14)

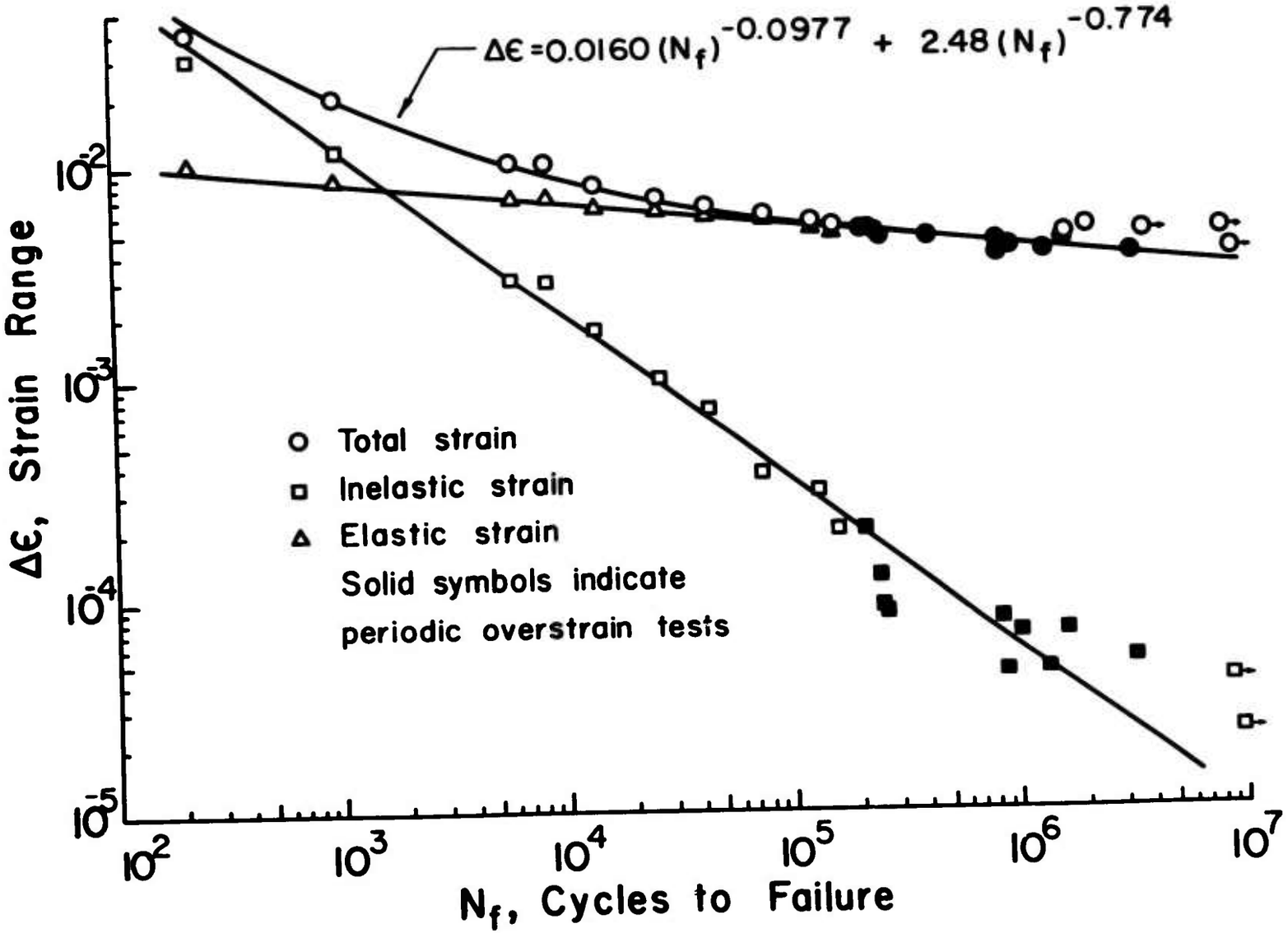

Fig. 16 Total Strain versus Life for SAE 4340 Steel (14)

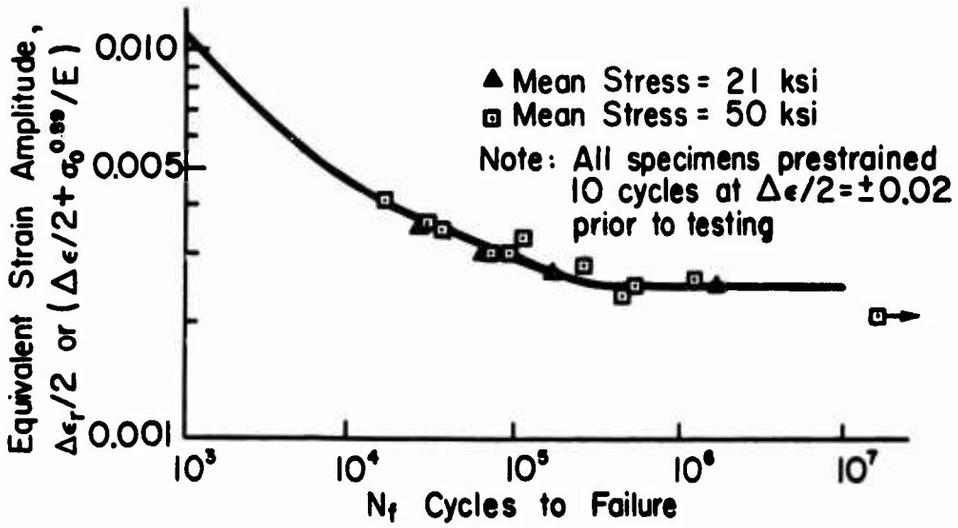

Fig. 17 Equivalent Strain Amplitude - Life Comparison for SAE 4340 Steel (10)

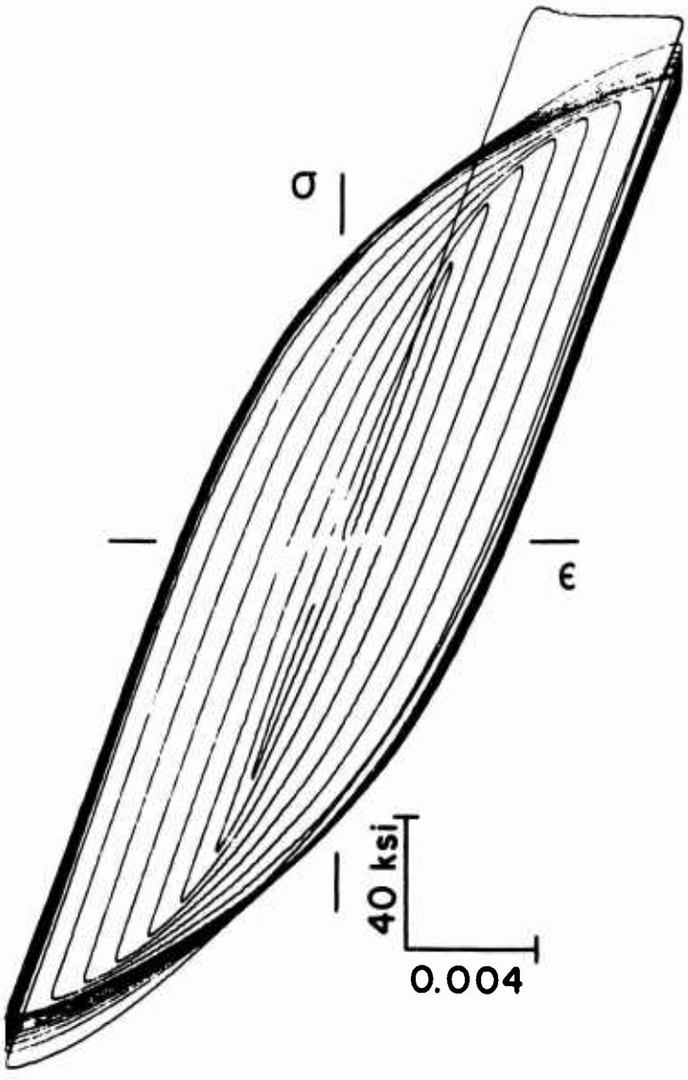

Fig. 18 Stress-Strain Recording for Initial Overstraining

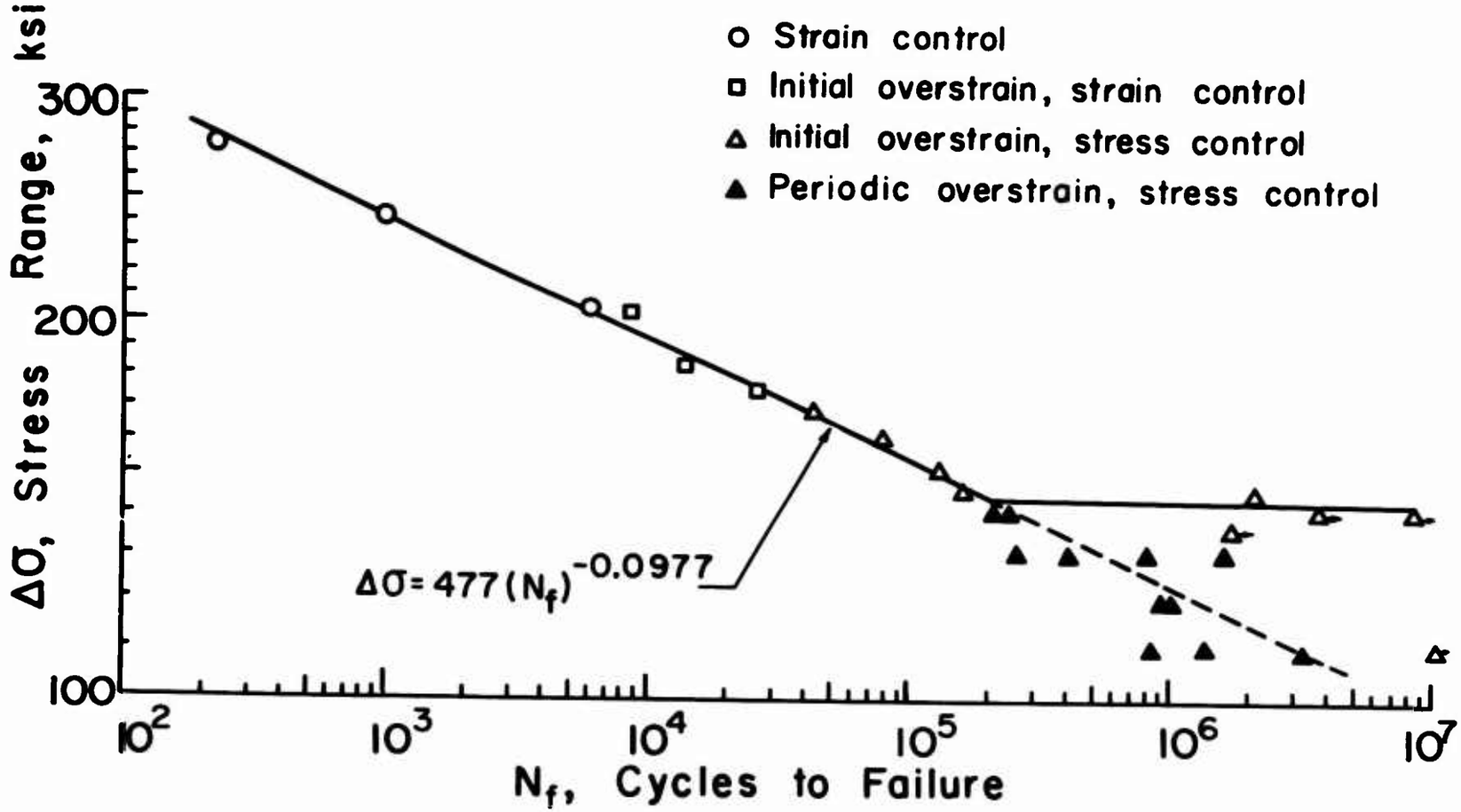

Fig. 19 Stress versus Life for SAE 4340 Steel (14)

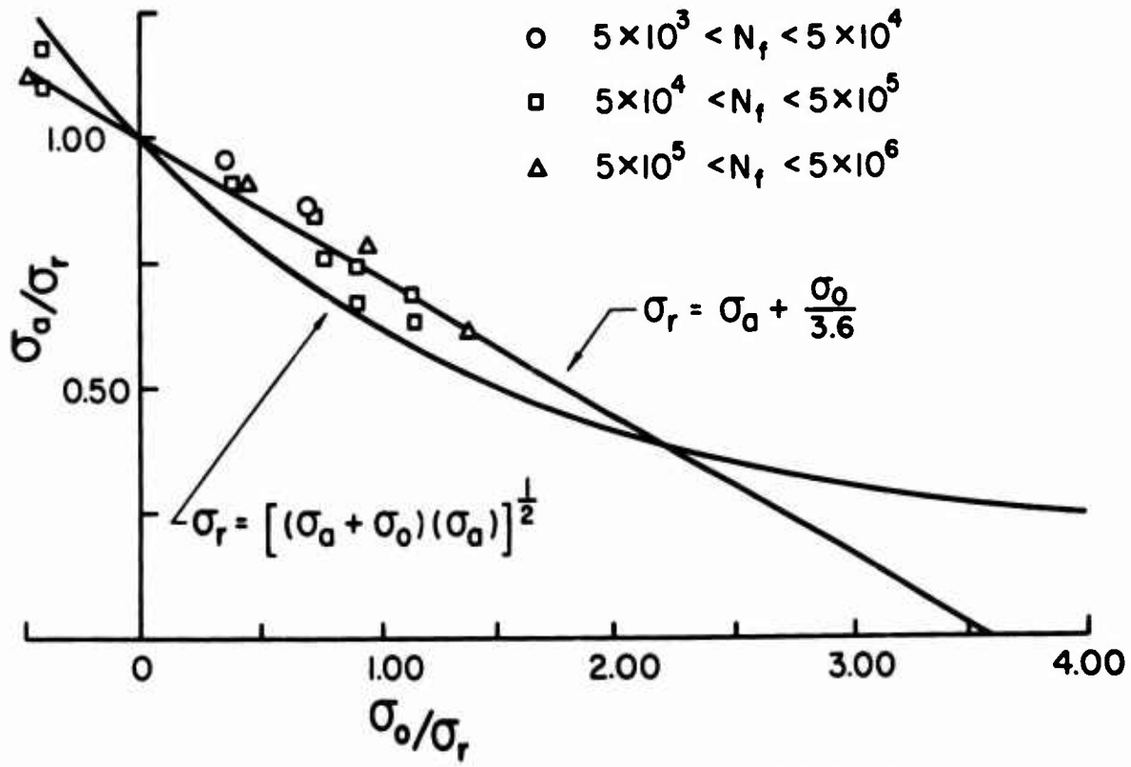

Fig. 20 Mean Stress Data for SAE 4340 Steel Compared to Eqs. 11 and 12

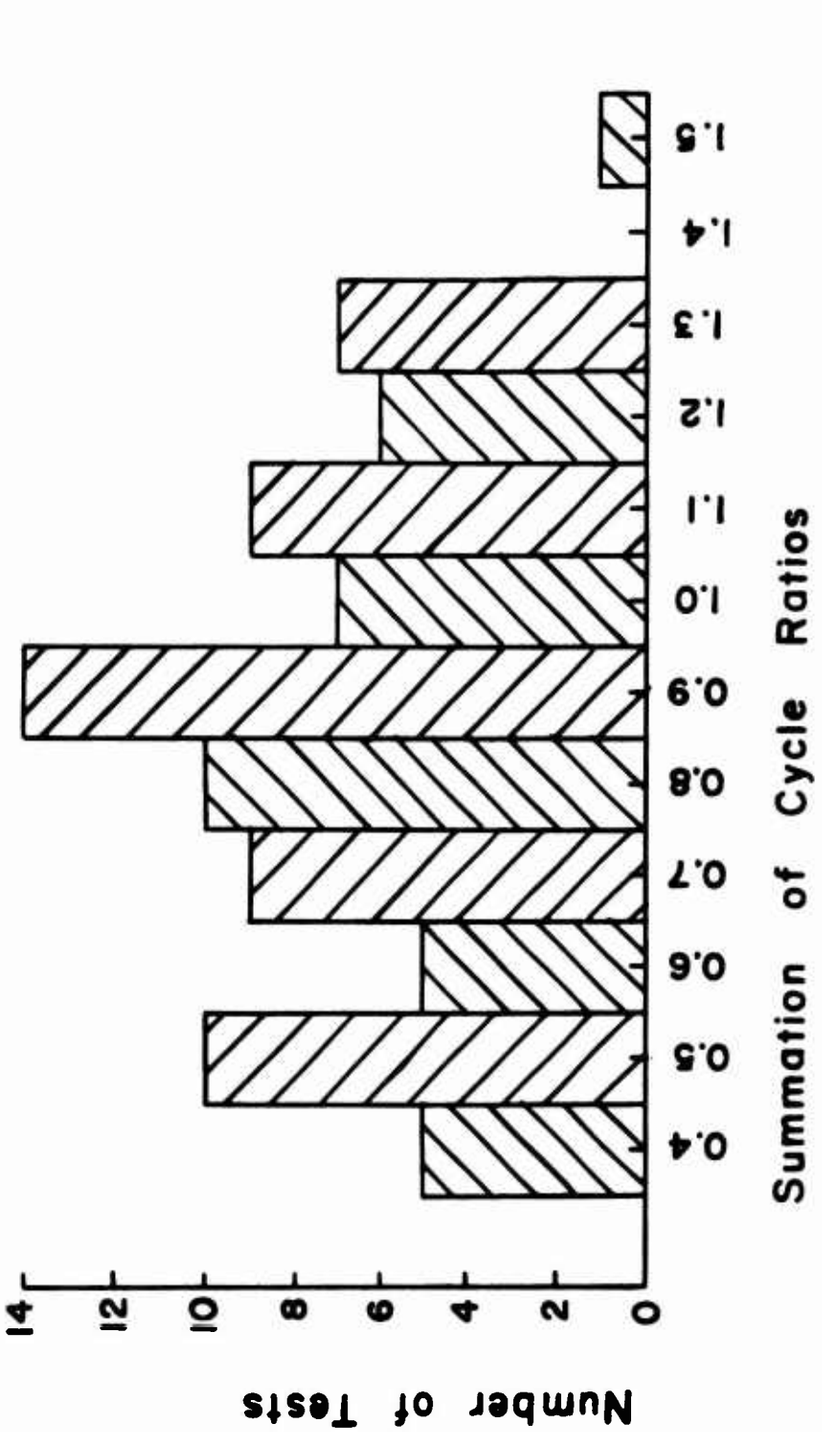

Fig. 21 Distribution of Failure Predictions for 2024-T4 Aluminum (15)

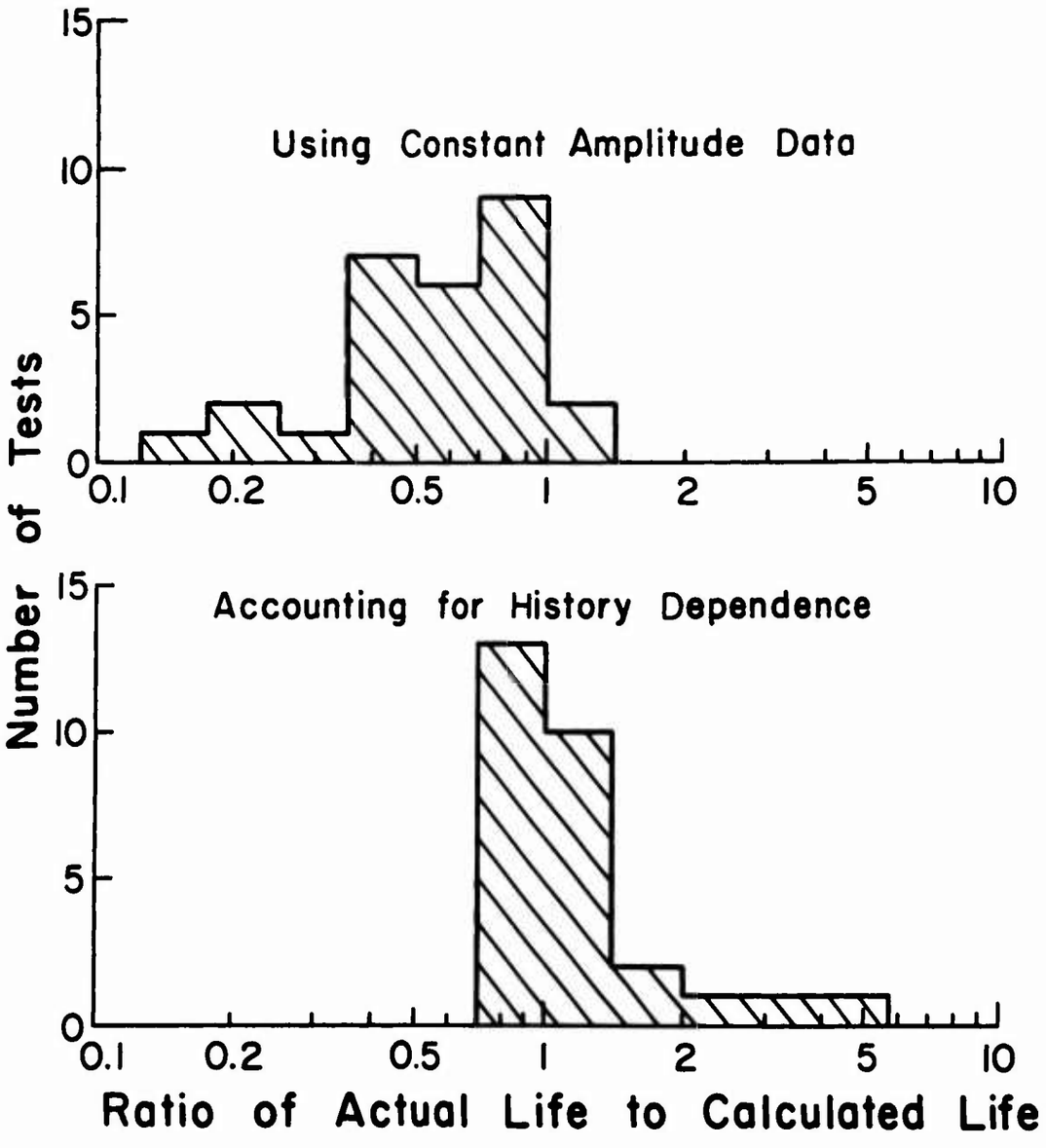

Fig. 22 Distributions of Life Calculations for SAE 4340 Steel(14)

One Block of Load Spectra

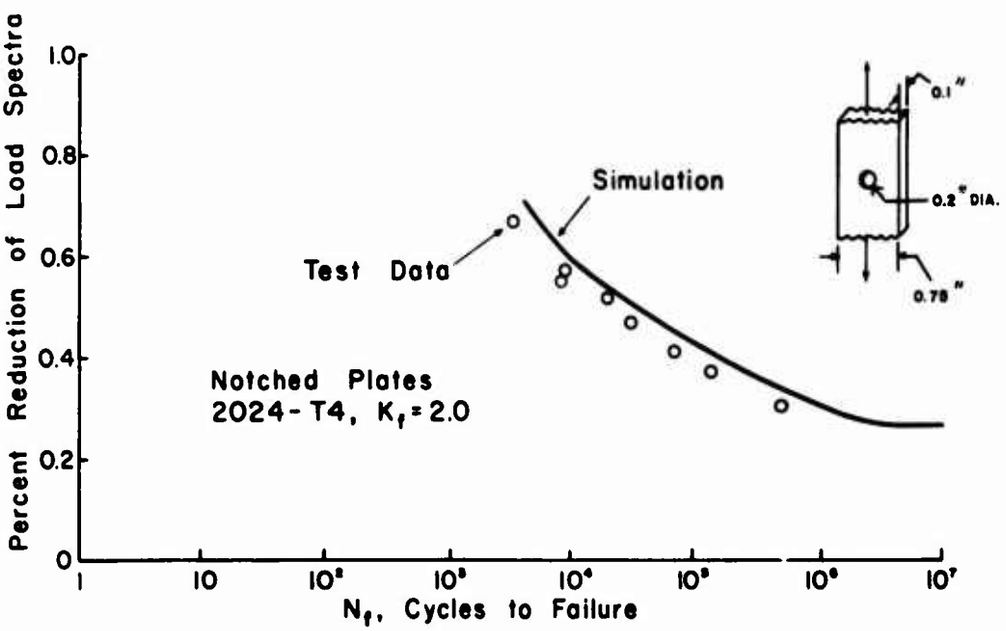

Fig. 23 Load-Life Curve for Plates Subjected to Load Spectra Shown (11)

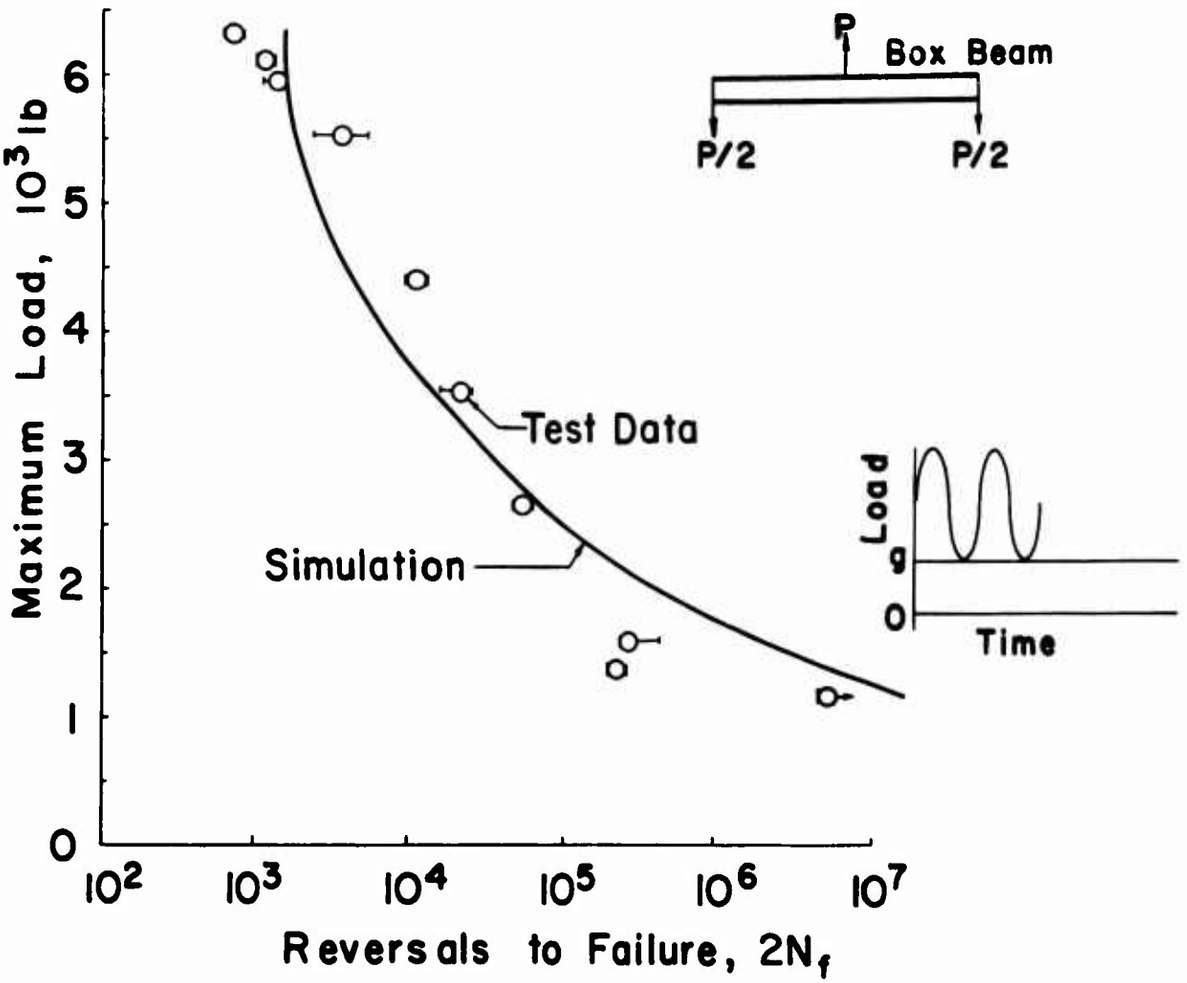

Fig. 24 Constant Amplitude Box Beam Predictions and Data: 1g to P_{max} Loading

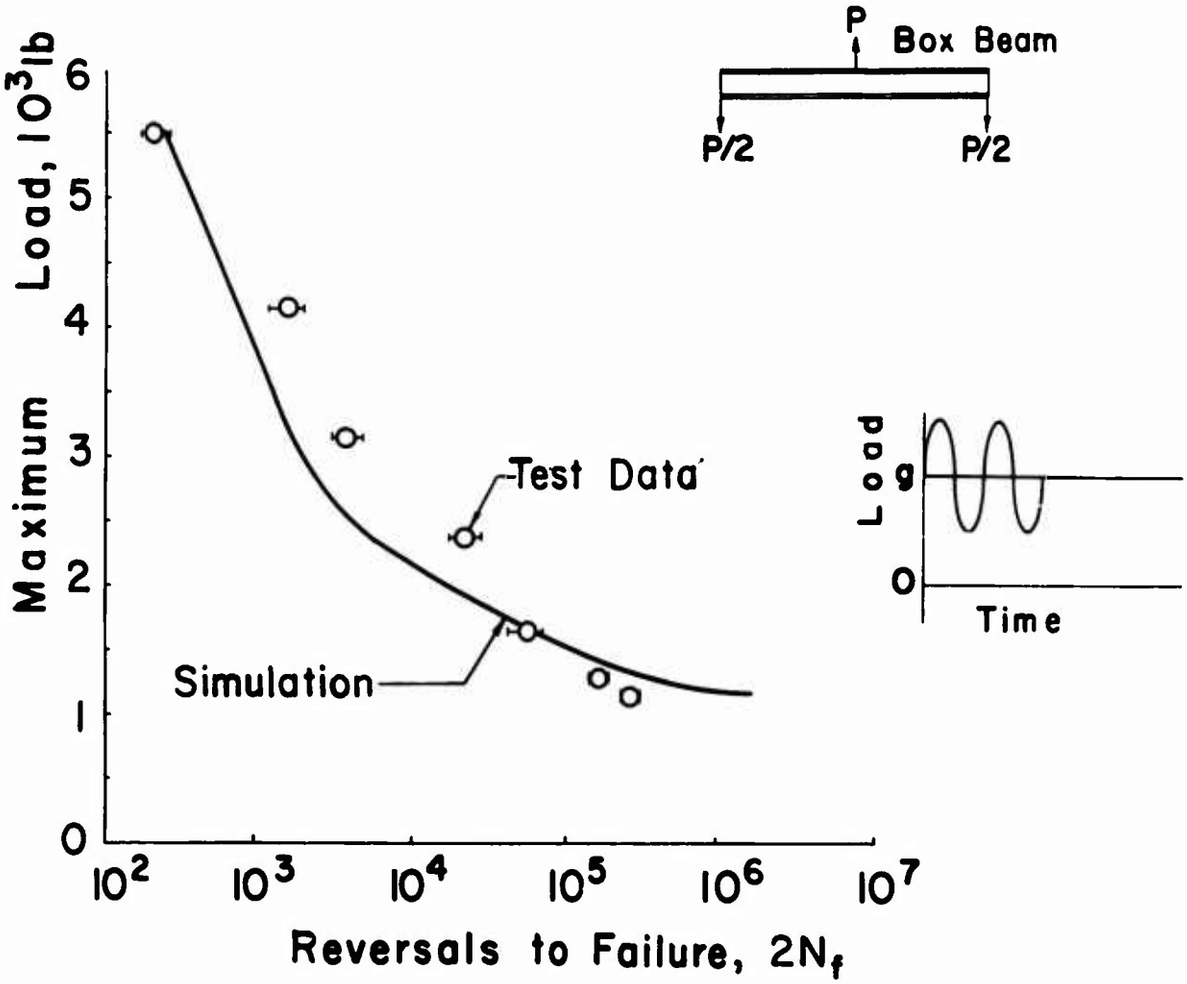

Fig. 25 Constant Amplitude Box Beam Predictions and Data: 1g ± P Loading

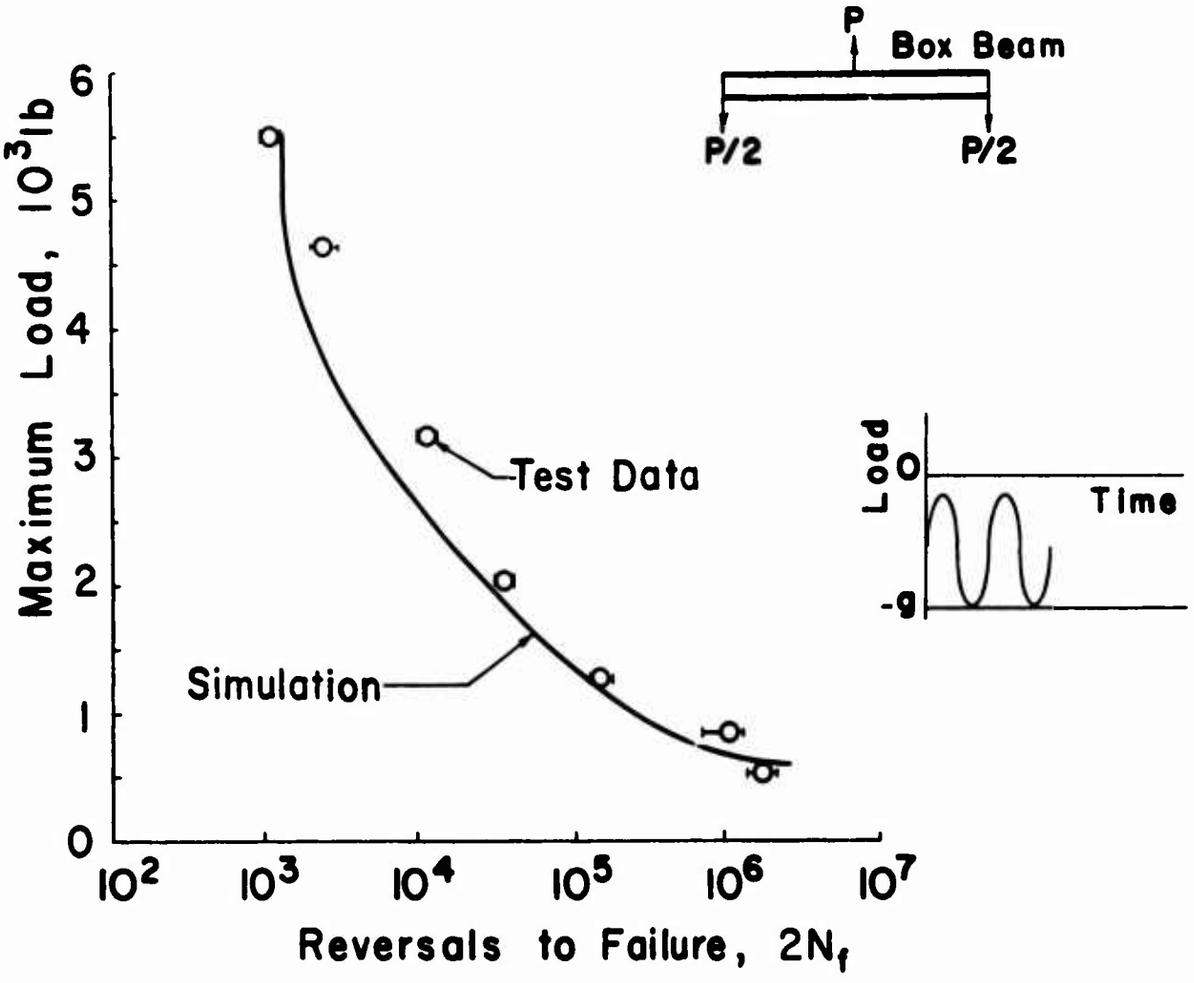

Fig. 26 Constant Amplitude Box Beam Predictions and Data: -1g to P_{max} Loading

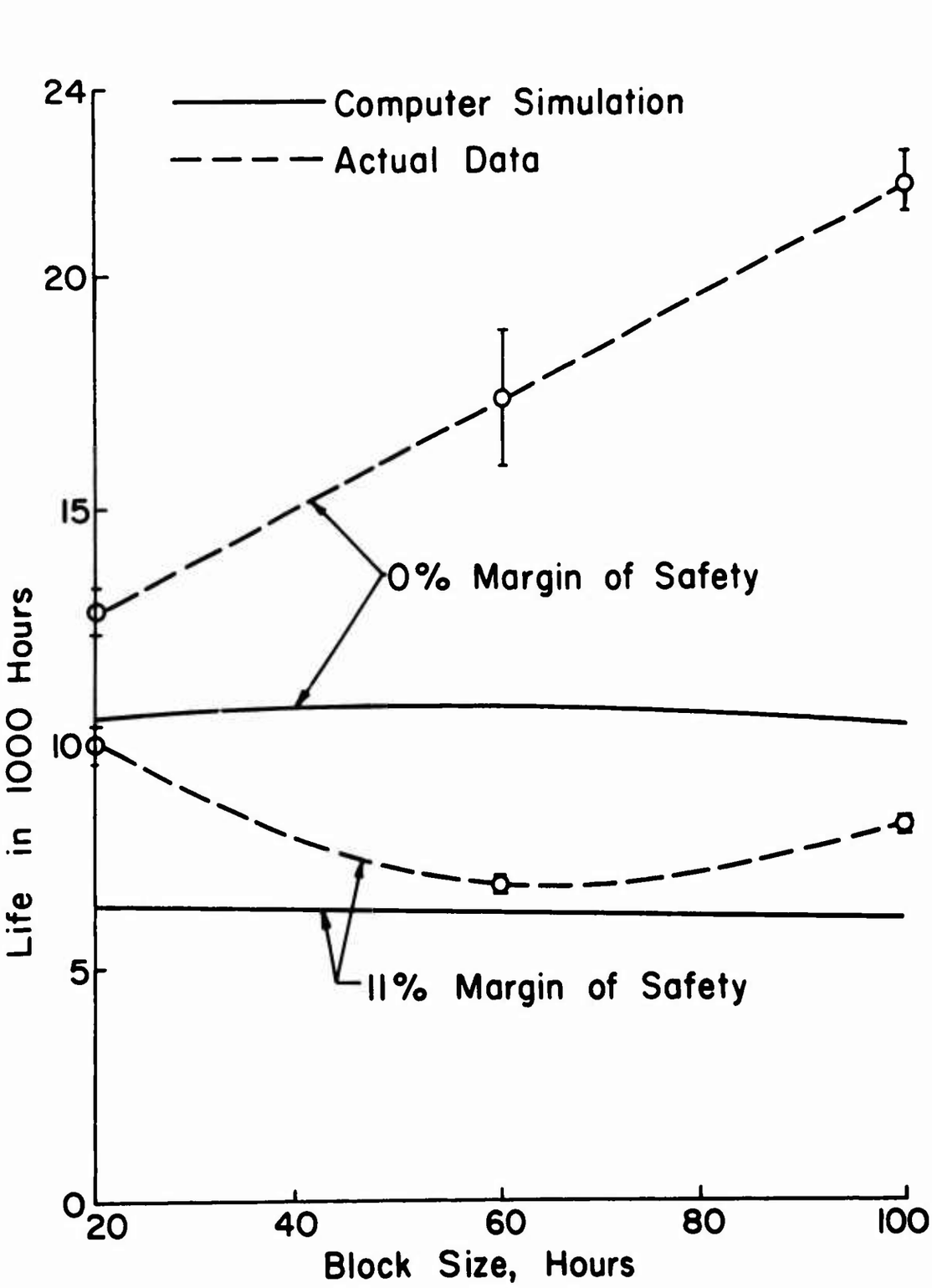

Fig. 27 Load Spectrum B Box Beam Predictions and Data

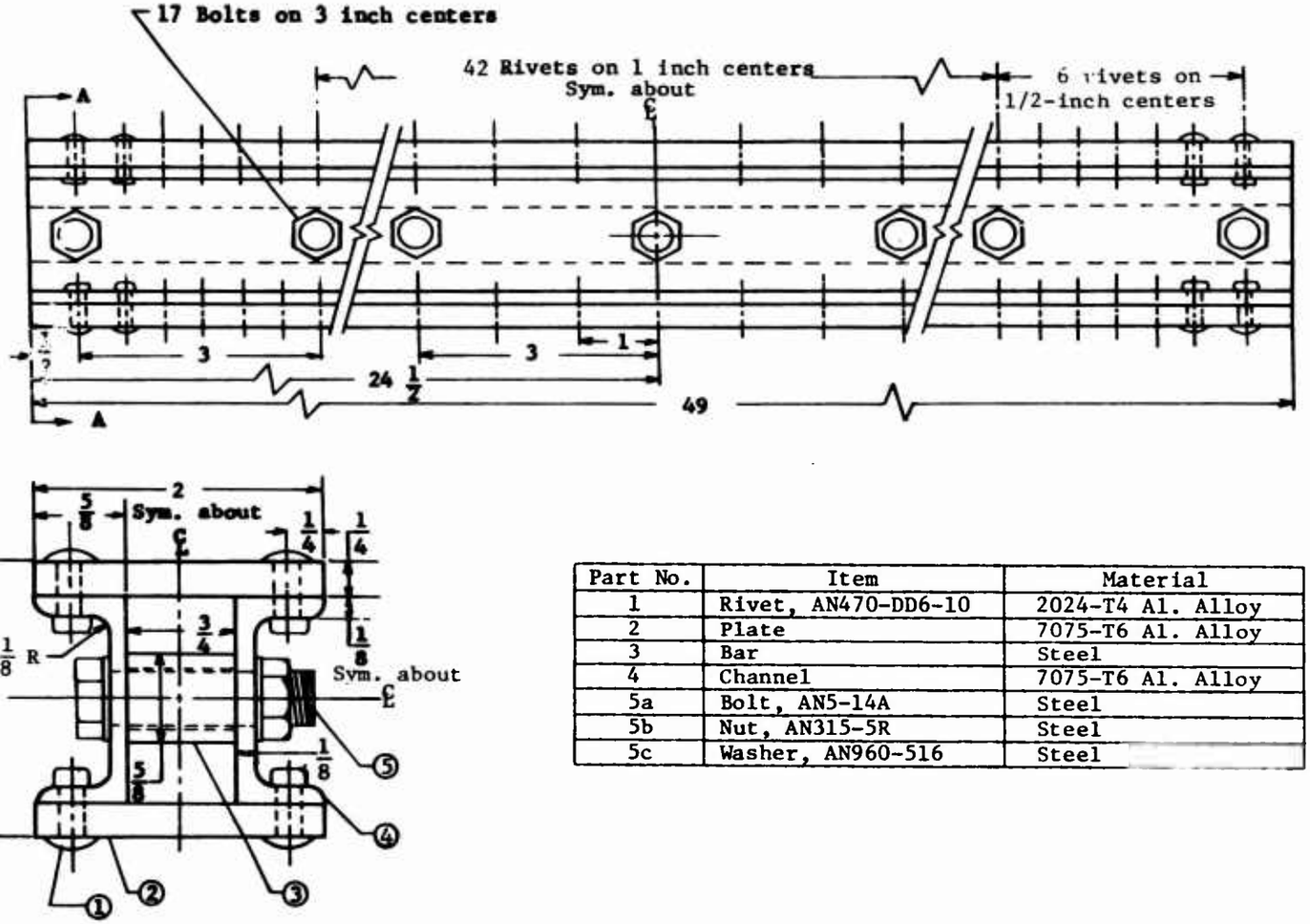

Part No.	Item	Material
1	Rivet, AN470-DD6-10	2024-T4 Al. Alloy
2	Plate	7075-T6 Al. Alloy
3	Bar	Steel
4	Channel	7075-T6 Al. Alloy
5a	Bolt, AN5-14A	Steel
5b	Nut, AN315-5R	Steel
5c	Washer, AN960-516	Steel

Fig. 28 Box Beam Specimen Design

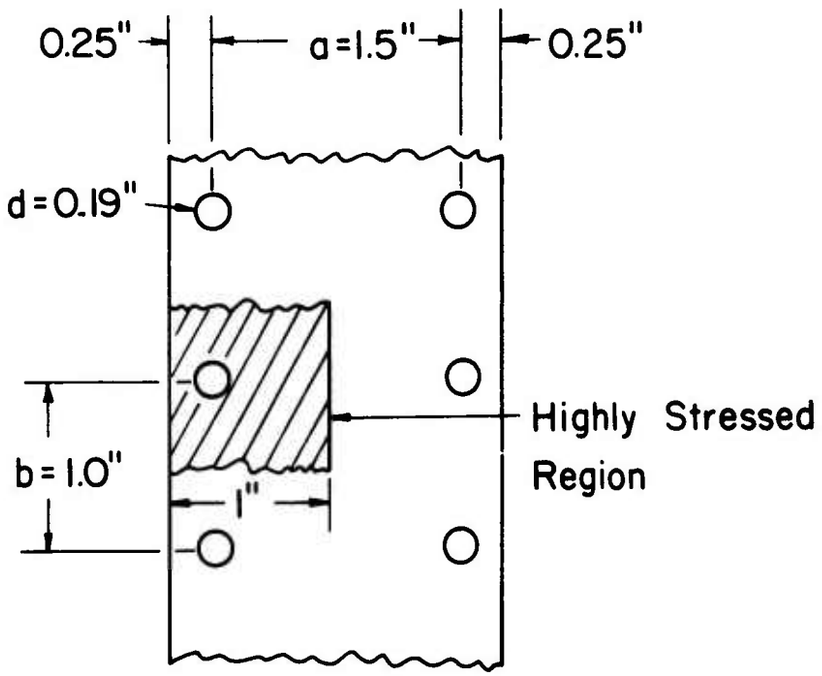

Fig. 29 Highly Stressed Area of Box Beam Cover Plate

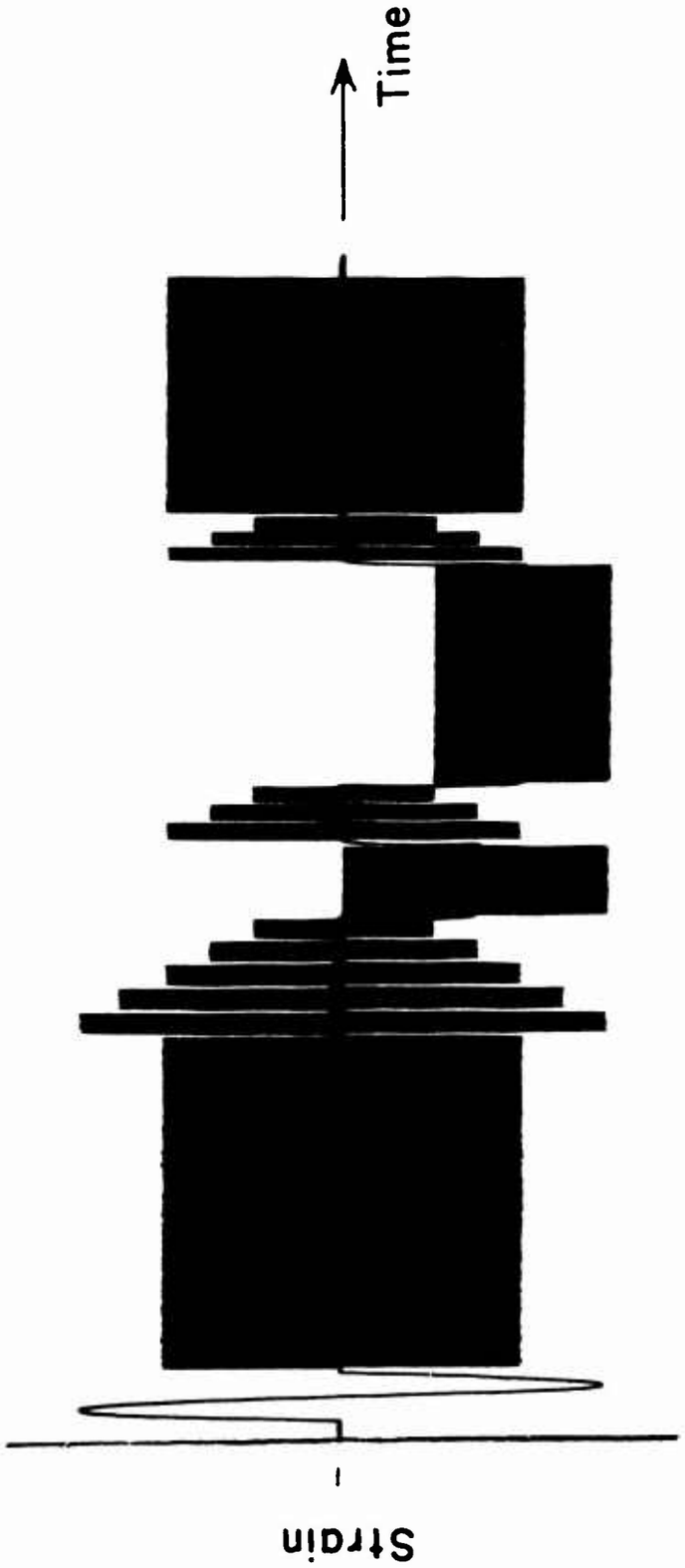

Fig. 30 Strain Spectrum for One Specimen Simulation

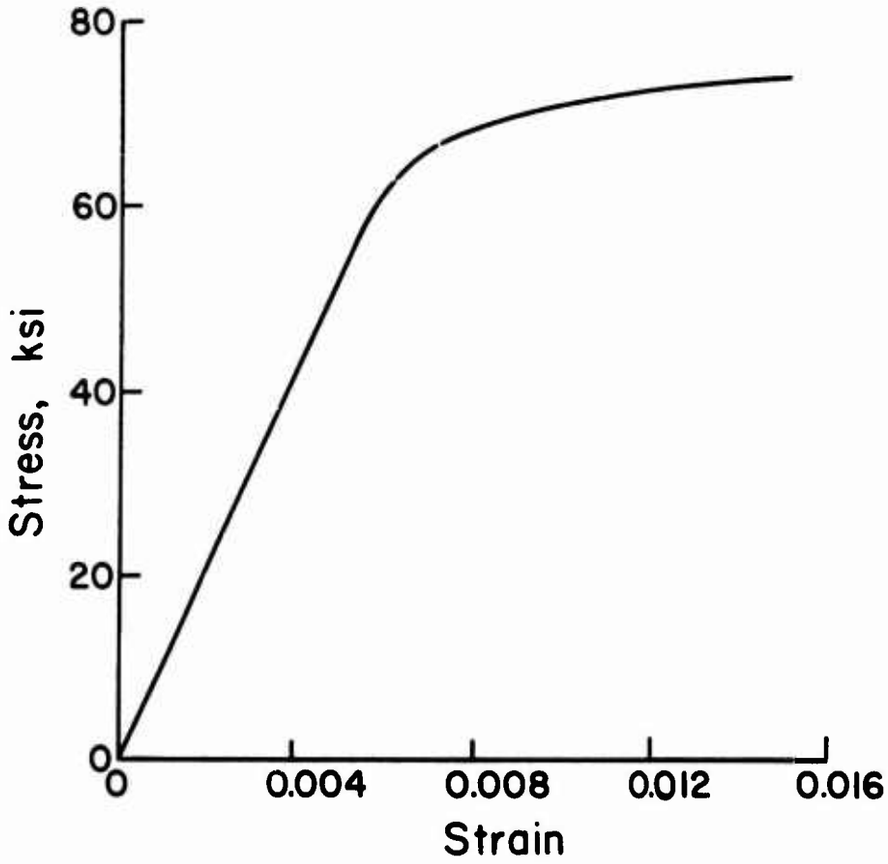

Fig. 31 Monotonic Stress-Strain Curve of 7075-T6 Aluminum

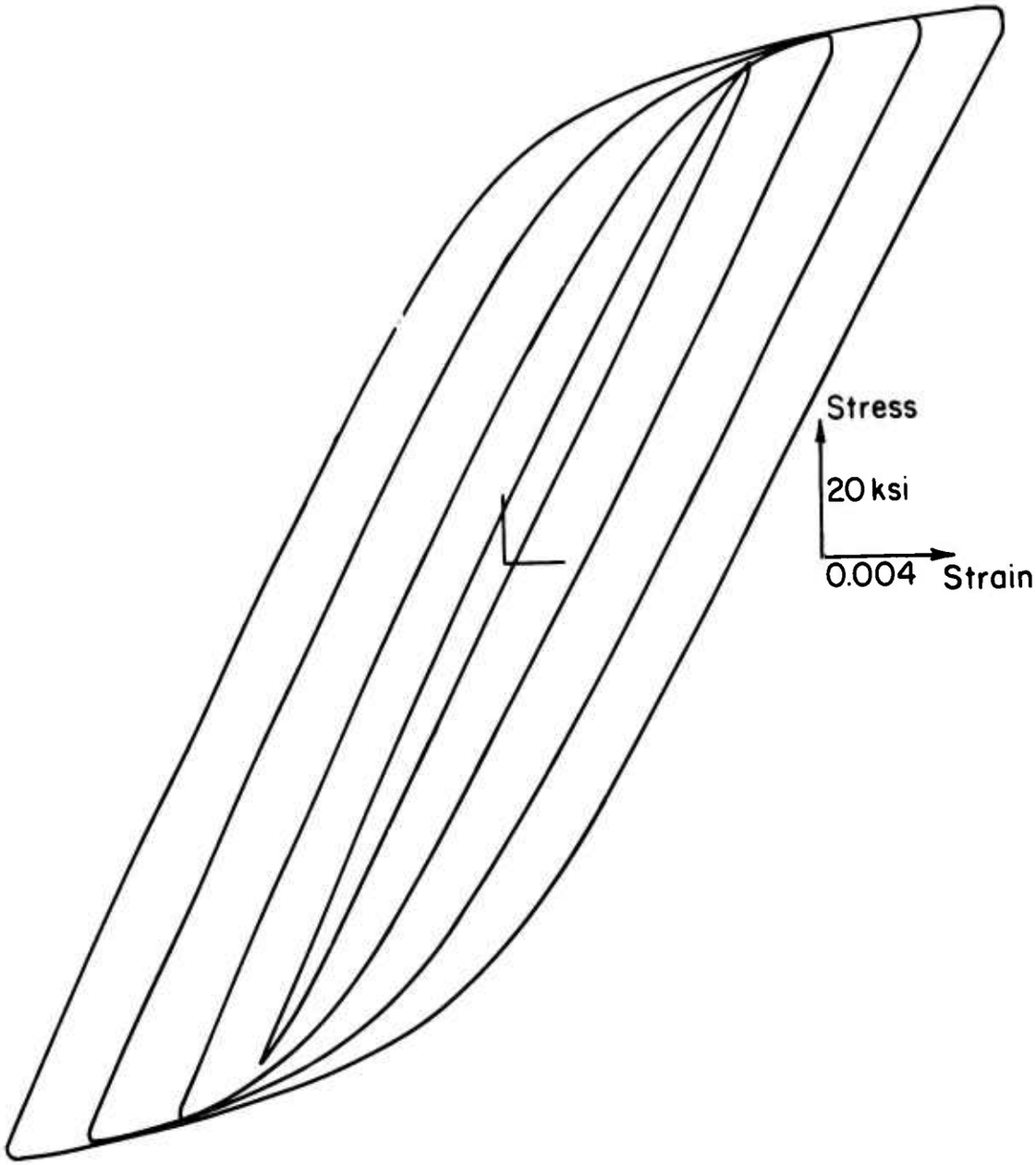

Fig. 32 Set of Stable Hysteresis Loops for Determining the Cyclic Stress-Strain Curve

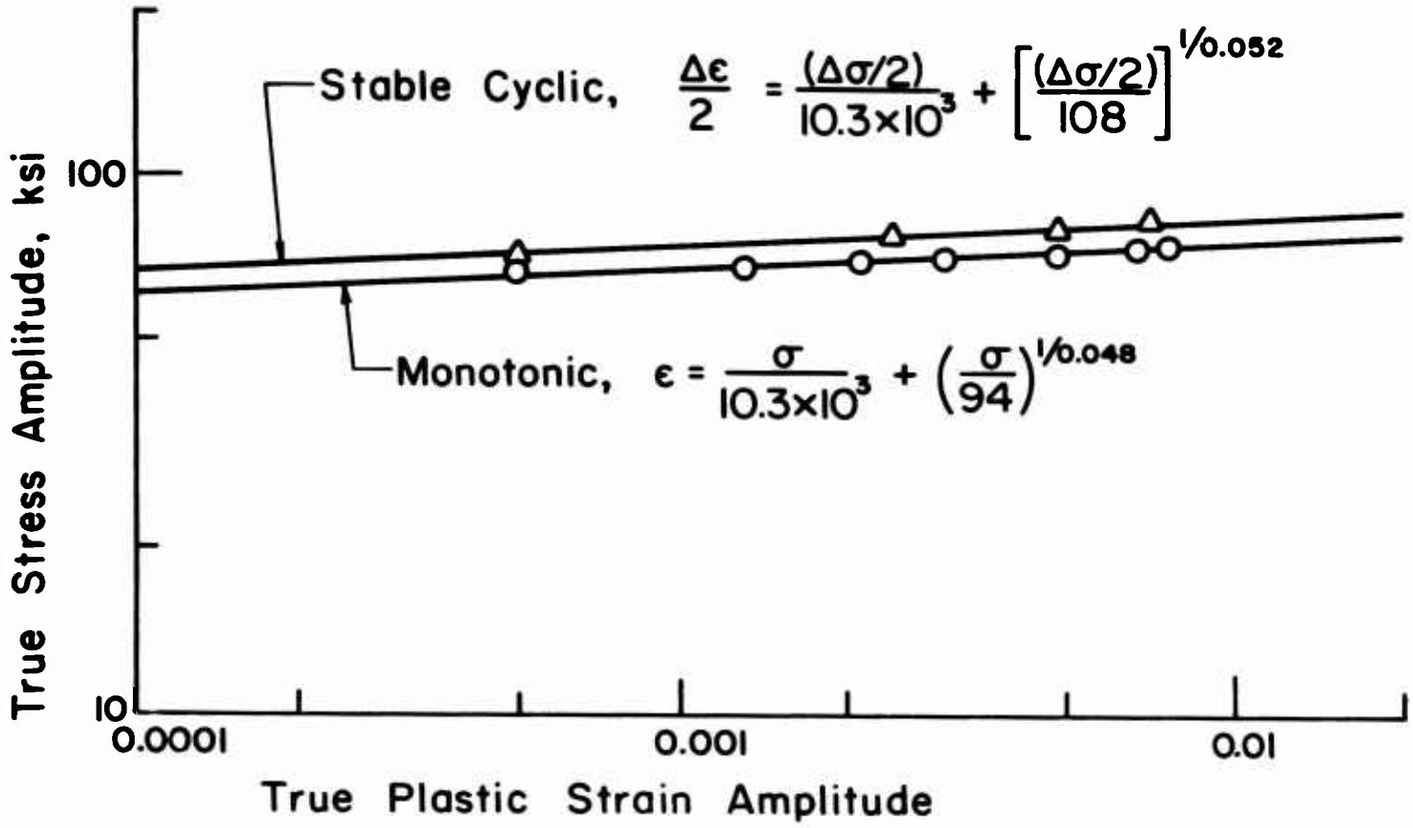

Fig. 33 Plastic Strain versus Stress Amplitude for 7075-T6 Aluminum

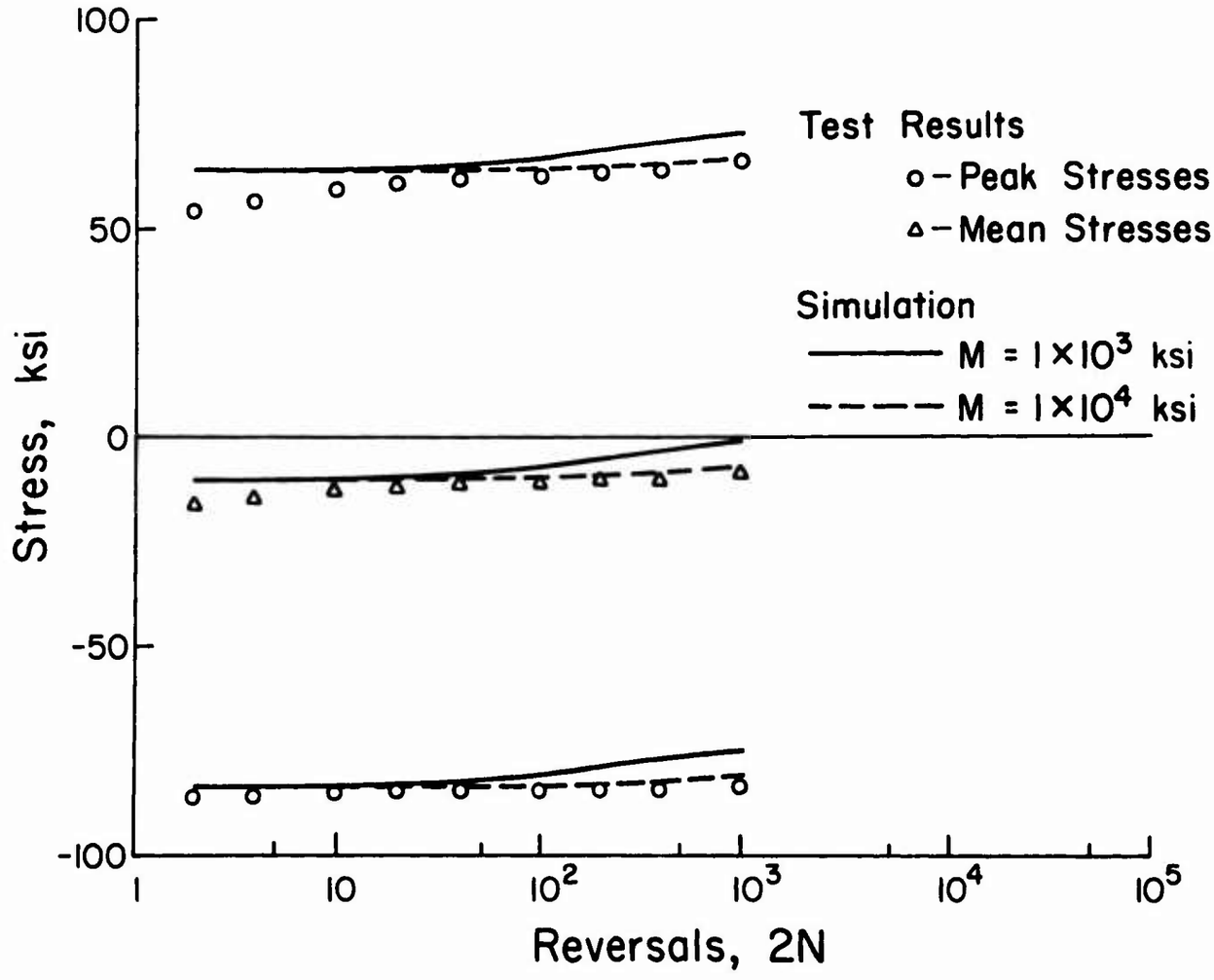

Fig. 34 Cyclic Relaxation Data for a Strain Range from 0.0 to -0.0155 for 7075-T6 Aluminum

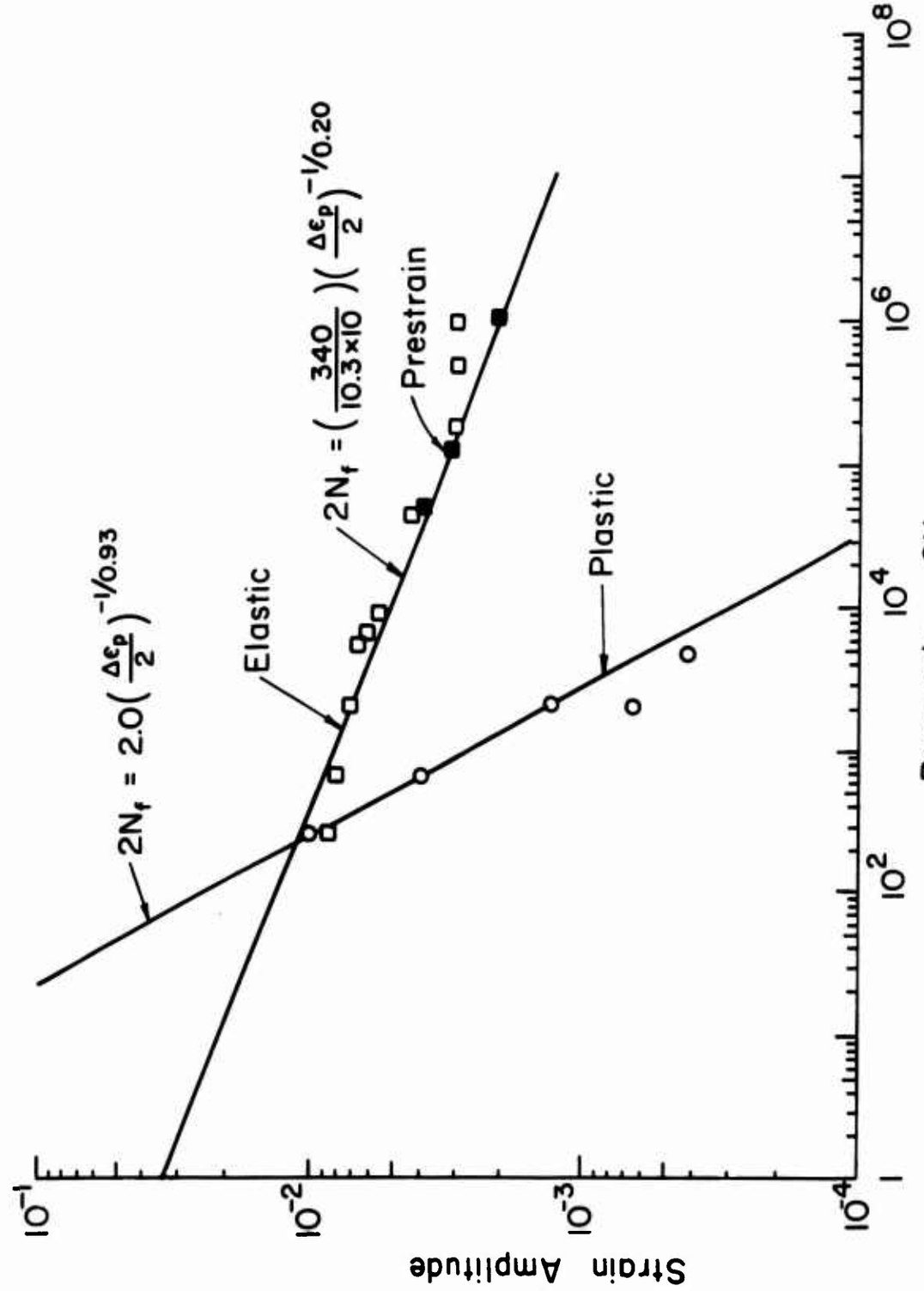

Fig. 35 Strain–Life Data for 7075-T6 Aluminum

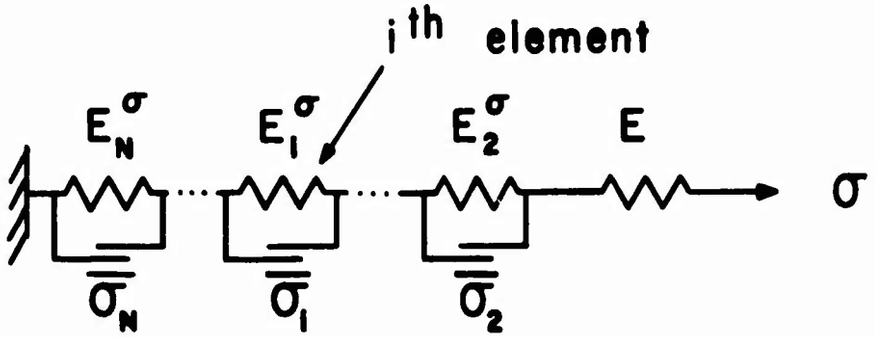

Fig. 36 Rheological Model for Computer Simulation

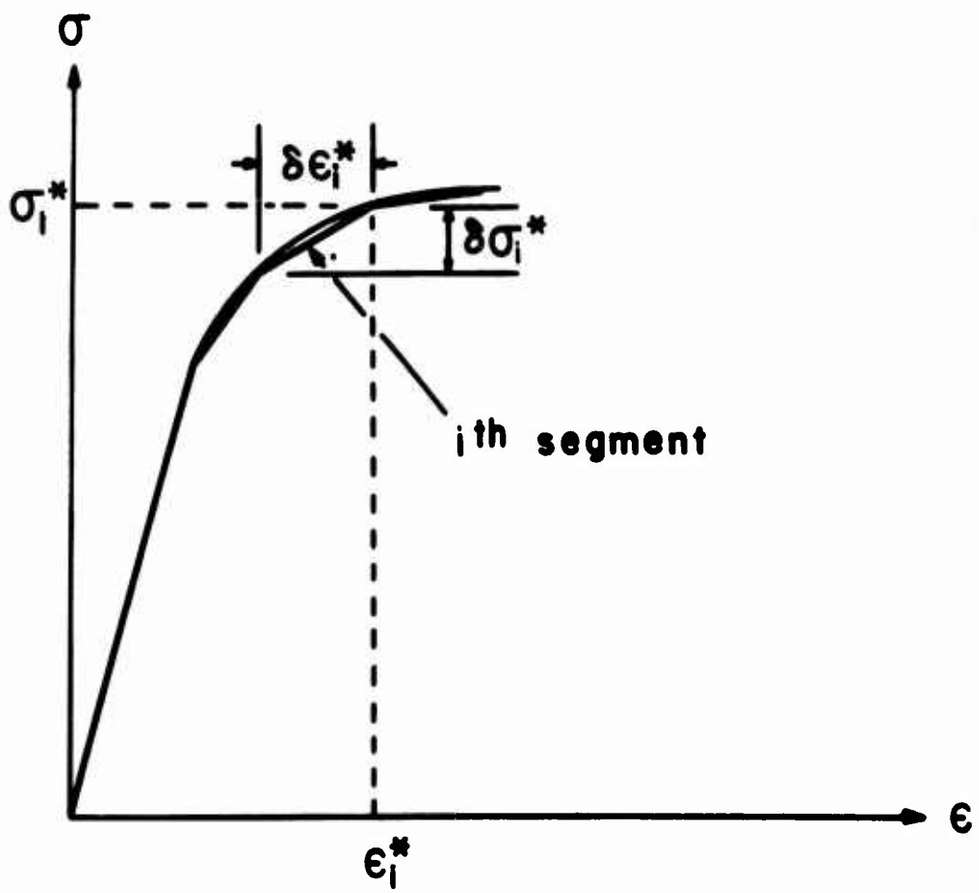

Fig. 37 Model Approximation of Stress-Strain Curve

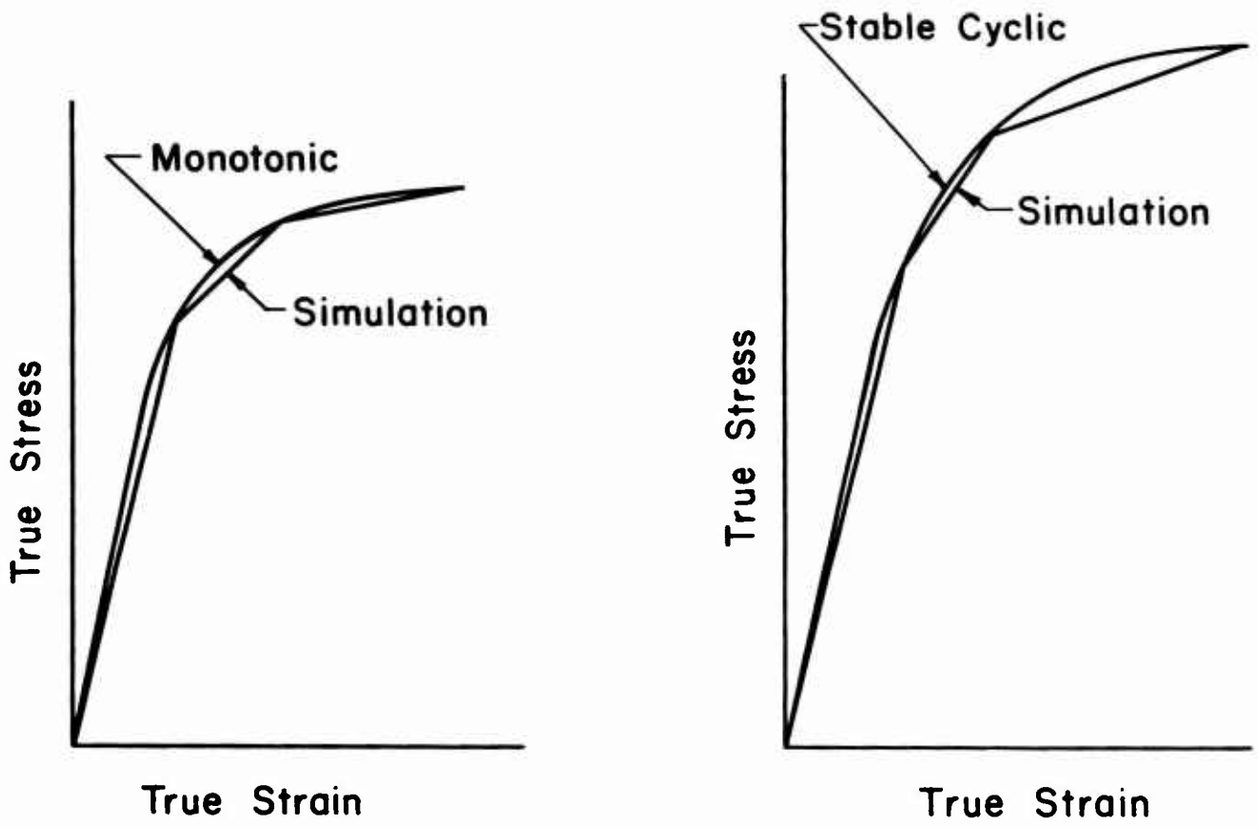

Fig. 38 Example of Cyclic Hardening Used in the Model

MAIN CHART

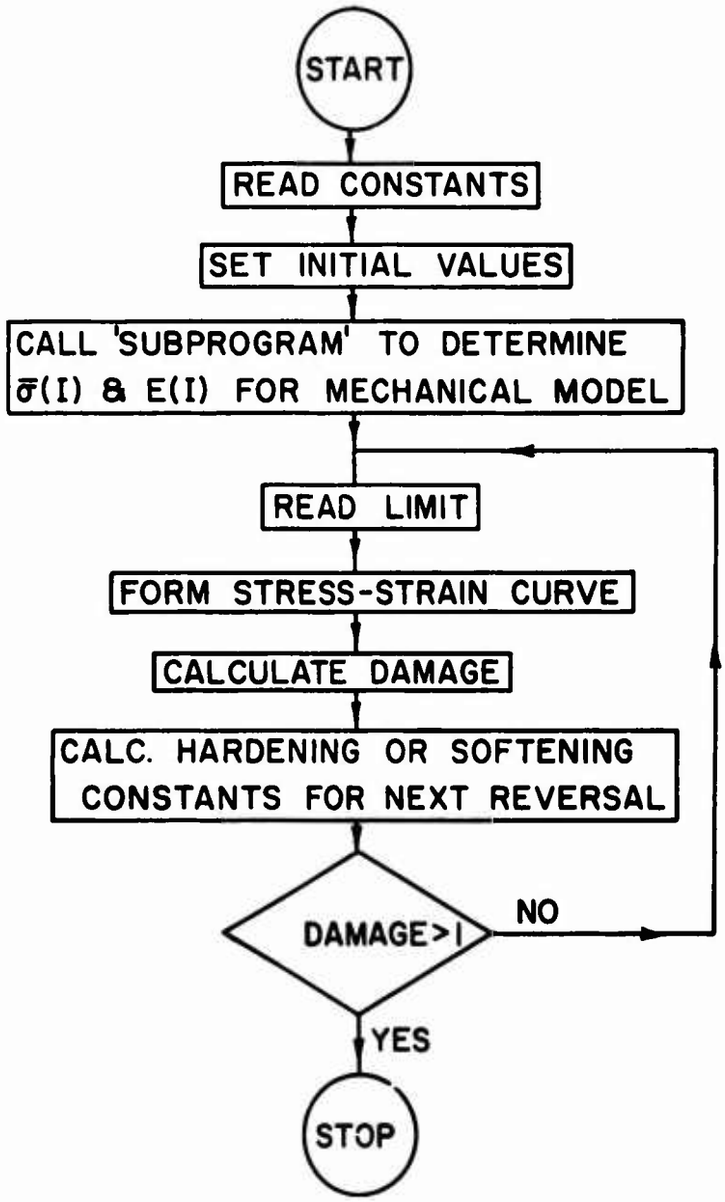

Fig. 39 Flow Chart of Computer Program